Published in : Journal of Medicinal Chemistry (2018), vol. 61, issue 12, pp. 5279-5291
doi.org/10.1021/acs.jmedchem.8b00250
Status : Postprint (Author's version)

ENHANCING ACTION OF POSITIVE ALLOSTERIC MODULATORS THROUGH THE DESIGN OF DIMERIC COMPOUNDS

Thomas Drapier,[†] Pierre Geubelle,[†,‡] Charlotte Bouckaert,[§] Lise Nielsen,[‖] Saara Laulumaa,[‖] Eric Goffin,[†] Sébastien Dilly [†] Pierre Francotte,[†] Julien Hanson,*[,†,‡] Lionel Pochet,*[,§] Jette Sandholm Kastrup,*[,‖] and Bernard Pirotte*[,†]

[†]*Laboratory of Medicinal Chemistry, Center for Interdisciplinary Research on Medicines (CIRM), ULiège, Quartier Hôpital, Avenue Hippocrate, 15, B36, B-4000 Liège, Belgium*
[‡]*Laboratory of Molecular Pharmacology, GIGA-Molecular Biology of Diseases, ULiège, B34, Quartier Hôpital, Avenue de l'hôpital, 11, B-4000 Liège, Belgium*
[§]*NAmur MEdicine & Drug Innovation Center (NAMEDIC), NARILIS, UNamur, rue de Bruxelles 61, B-5000 Namur, Belgium*
[‖]*Biostructural Research, Department of Drug Design and Pharmacology, Faculty of Health and Medical Sciences, University of Copenhagen, Universitetsparken 2, DK-2100 Copenhagen, Denmark*

* Supporting Information

Abstract

The present study describes the identification of highly potent dimeric 1,2,4-benzothiadiazine 1,1-dioxide (BTD)-type positive allosteric modulators of the AMPA receptors (AMPApams) obtained by linking two monomeric BTD scaffolds through their respective 6-positions. Using previous X-ray data from monomeric BTDs cocrystallized with the GluA2 ligand-binding domain (LBD), a molecular modeling approach was performed to predict the preferred dimeric combinations. Two 6,6-ethylene-linked dimeric BTD compounds (16 and 22) were prepared and evaluated as AMPApams on HEK293 cells expressing GluA2$_o$(*Q*) (calcium flux experiment). These compounds were found to be about 10,000 times more potent than their respective monomers, the most active dimeric compound being the bis-4-cyclopropyl-substituted compound 22 [6,6'-(ethane-1,2-diyl)bis(4-cyclopropyl3,4-dihydro-2*H*-1,2,4-benzothiadiazine 1,1-dioxide], with an EC50 value of 1.4 nM. As a proof of concept, the bis-4-methylsubstituted dimeric compound 16 (EC_{50} = 13 nM) was successfully cocrystallized with the GluA2$_o$-LBD and was found to occupy the two BTD binding sites at the LBD dimer interface.

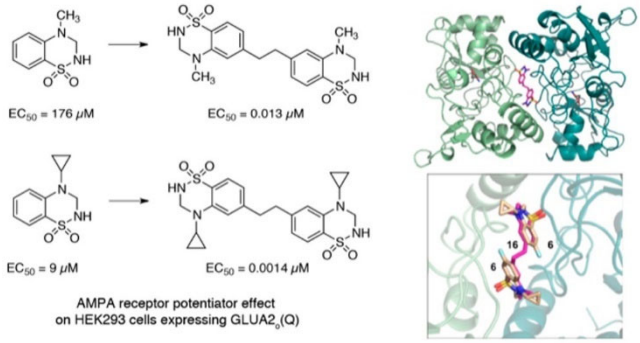

Published in : Journal of Medicinal Chemistry (2018), vol. 61, issue 12, pp. 5279-5291
doi.org/10.1021/acs.jmedchem.8b00250
Status : Postprint (Author's version)

Introduction

It is well established that L-glutamate is the key excitatory neurotransmitter in the central nervous system (CNS).[1] L-Glutamate exerts its biological effect on the CNS through the activation of either metabotropic (mGluRs, G protein-coupled) or ionotropic (iGluRs, ligand-gated ion channel) receptors.[1,2] iGluRs can be classified into three subcategories depending on their affinity toward nonendogenous ligands: N-methyl-D-aspartic acid (NMDA) receptors, *α*-amino-3-hydroxy-5-methyl-4-isoxazolepropionic acid (AMPA) receptors, and kainic acid (KA) receptors.[1,2] Due to rapid response to L -glutamate in the synapses, iGluRs play a sustainable role in the fast transmission of excitatory potentials from one neuron to another.[3–5] Several studies have shown the impact of a decrease of the AMPA signaling in brain disorders such as attention deficit hyperactivity disorder (ADHD), Alzheimer's disease, mild depression, or schizophrenia.[6–8] Based on this, the AMPA receptors (AMPARs) seem to be an interesting pharmacological target for the development of either probing tools or cognitive enhancers.

It is conceivable that agonists could be used as cognitive enhancers, but their development is questioned due to the possible occurrence of unwanted and adverse phenomena related to excitotoxicity.[9] Therefore, AMPA positive allosteric modulators (so-called "AMPApams") have been postulated to be a more promising option. Because they do not bind into the orthosteric-binding site but into an allosteric binding site, they are expected to be devoid of an intrinsic activity on the AMPARs and to show an effect only when glutamate is released in the synapse. This mode of action is assumed to give better fine-tuning of the AMPA receptor signaling and to avoid the excitotoxicity problems resulting from overdose of a direct agonist.

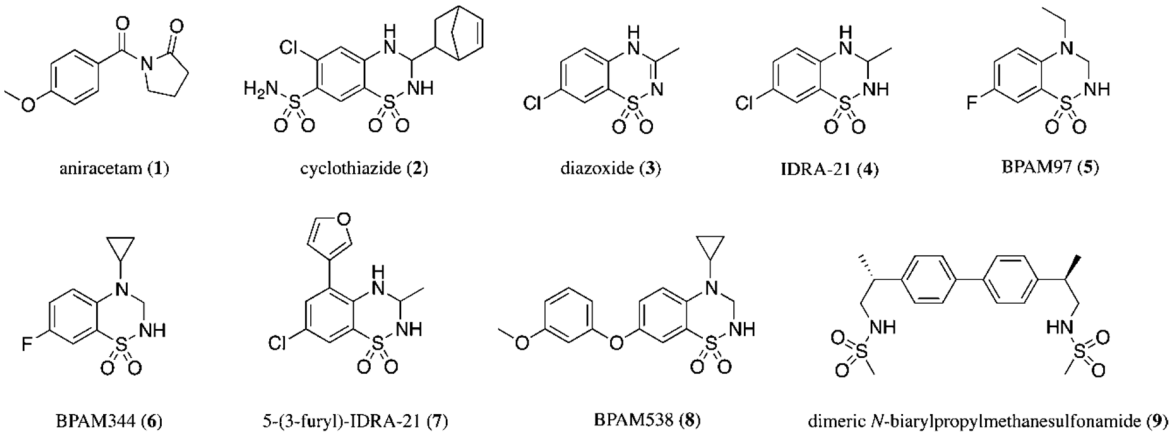

Figure 1. Known AMPA receptor modulators from different families. Benzamides, (1) aniracetam; 1,2,4-benzothiadiazine 1,1-dioxides, (2) cyclothiazide, (3) diazoxide, (4) IDRA-21, (5) BPAM97, (6) BPAM344, (7) 5-(3-furyl)-IDRA-21,[58] (8) BPAM538; N-biarylpropyl- methanesulfonamides, dimeric compound (9)

Published in : Journal of Medicinal Chemistry (2018), vol. 61, issue 12, pp. 5279-5291
doi.org/10.1021/acs.jmedchem.8b00250
Status : Postprint (Author's version)

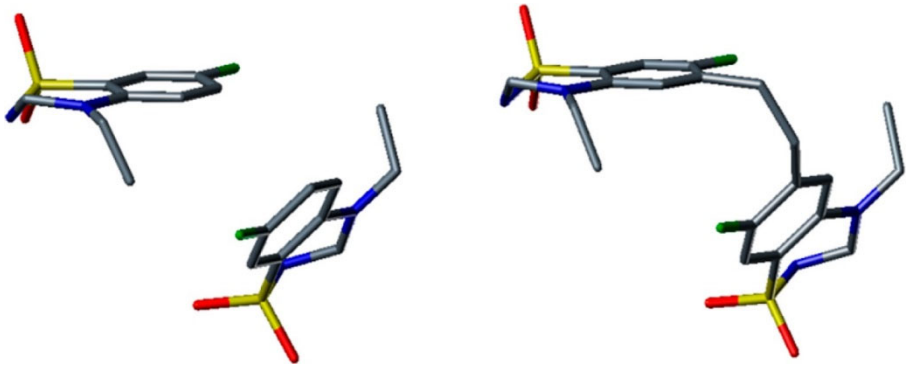

Figure 2. Spatial arrangement of two molecules of 5 at the interface of two GluA2 LBDs (left) according to the cocrystallization data.[28] Spatial arrangement of modeled dimeric compound 5 linked with an ethylene bridge at the 6-position of each benzothiadiazine dioxide scaffold [modeled under the SYBYL 8.0 software (Tripos Inc.: St. Louis, MO, 2008)] by using a library of standard fragments; the geometry was then optimized using the MMFF94 force field.[59] It was expected that the dimeric compound can adopt a conformation that fits the two binding sites of the two constitutive monomers.

AMPARs consist of various combinations of four different subunits (GluA1−4) that can bind to each other in several ways, either on a homo- or a heteromeric scaffold with heteromeric constructions preferred in wild type neurons.[10] They first assemble in dimers and then in functional dimers of dimers (homodimers or heterodimers).[11] Each subunit constituting the receptors can be divided into four semiautonomous domains.[12−14] Two of them are extracellular: the amino-terminal domain (ATD) and the ligand-binding domain (LBD). One is inside the membrane, which constitutes the channel itself, the transmembrane domain (TMD). The last one is intracellular, the carboxy-terminal domain (CTD).[12−14] Interactions with ligands occur at the level of the LBD, either with L-glutamate or with different allosteric modulators, respectively, in the orthosteric (agonist) binding site and in the allosteric binding site, which lies at the interface of two subunits.[2] The interactions of AMPApams with the AMPAR can lead to two main outcomes: they can act on slowing down the receptor deactivation process by enhancing the affinity of L-glutamate for its orthosteric binding site or they can increase the affinity between subunits, thereby inhibiting the receptor desensitization process, where conformational changes lead to the closure of the channel even if L-glutamate is still bound.[15−17]

The well-known allosteric binding site has a U shape and comprises LBDs of both subunits. It is divided in three smaller subsites called A, B/B', and C/C'.[18,19] Allosteric modulators interact with the different subsites depending on their chemical structure. For example, the benzamide-type family of AMPApams was shown to interact mostly with the A subsite.[18] Among those compounds, aniracetam (1, Figure 1) is referred to as the oldest molecule acting as an AMPApam.[20] The second major chemical class of AMPApams is the ring-fused thiadiazine family of compounds among which the benzothiadiazine dioxide (BTD) members are the most prominent representatives.20 They were studied following the discovery of the in vitro AMPAR potentiation by cyclothiazide (2, Figure 1), a compound used in clinical practice for its diuretic action.[21] However, this drug did not show marked *in vivo* activity on the CNS resulting from AMPAR potentiation, probably because of its inability to cross the blood−brain barrier (BBB).[18,20] Cyclothiazide interacts with the B and C subsites of this allosteric binding site in a symmetrical way resulting in an interaction of one molecule per subunit, thus two molecules at the dimer interface.[18] Unlike cyclothiazide, IDRA 21 (4, Figure 1), a saturated analog of the potassium channel opener diazoxide (3, Figure 1), was found to be active *in vitro* as an AMPApam[22] and was further identified *in vivo* as a cognitive enhancer in animal models of cognitive impairments.[23,24].

Published in : Journal of Medicinal Chemistry (2018), vol. 61, issue 12, pp. 5279-5291
doi.org/10.1021/acs.jmedchem.8b00250
Status : Postprint (Author's version)

Accordingly, many examples of ring-fused thiadiazine dioxides based on this structure were developed as AMPApams (see, for example, compounds 5−8; Figure 1).[20,25] These molecules interact in different ways with the binding site compared to cyclothiazide: being smaller, they rotate in the cavity and only interact with the hydrophobic C/C′ subsites (still with a ratio of one molecule per subunit, thus two molecules per dimer interface).[18] Recently, the large-sized BTD modulator 8 (BPAM538) was found to bind the "BTD" allosteric site with a high affinity and with only one molecule per dimer interface.[26] Other families of AMPApams that have their own way to interact with the allosteric binding site have been reported,[20] among which are *N*-biaryl(cyclo)alkyl-2-propanesulfonamides, phenyliminothiazoles, and 3-trifluoromethylpyrazoles.

Among the reported AMPApams, N-biarylpropylmethanesulfonamides such as 9 synthesized by Kaae et al.[27] should be highlighted as the first examples of dimeric molecules modulating the activity of AMPARs. The authors showed that some dimeric compounds acted as AMPApams with a drastic 1000-fold elevation of the potency compared to the constitutive monomers.[27] This gain of potency was tentatively explained by the presence of the 2-fold pattern fitting in the two subsites, C and C′, on both sides of the AMPAR dimer interface.

Table 1. Proposed Dimeric Structures for the Docking Studies with Their Occurrence, ChemPLP Score, and Calculated Binding Energy (BE)

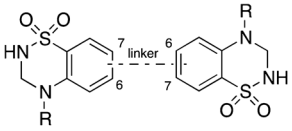

A-D ; G-J

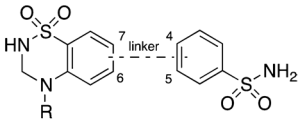

E, F

numbering	linker	R	occurrence[a]	ChemPLP score	BE (kcal/mol)
A or 16	6-$(CH_2)_2$-6	methyl	20/20	84.0	−55.7
B or 22	6-$(CH_2)_2$-6	cyclopropyl	11/20	90.2	−54.8
C	6-$(CH_2)_3$-6	methyl	13/20	87.8	−45.4
D	6-$(CH_2)_3$-6	cyclopropyl	10/20	90.1	−53.2
E	6-$(CH_2)_2$-4	cyclopropyl	18/20	78.1	−26.9
F	6-$(CH_2)_2$-4	cyclopropyl	9/20	81.0	−34.6
G	7-$(CH_2)_2$-7	methyl	20/20	85.1	−25.0
H	7-$(CH_2)_2$-6	methyl	11/20	78.1	−37.3
I	6-NH−CO-6	methyl	13/20	61.4	−2.74
J	6-NH−CH_2-6	methyl	15/20	81.1	−50.3

[a] The selected docking pose is the best representative (based on the ChemPLP score) of the cluster having the highest occurrence. In this study, the selected docking poses are, in addition, the best docking poses among the 20 solutions given by Gold except for dimeric compounds C and F.

Based on X-ray data obtained from some examples of BTDtype AMPApams synthesized by our team and cocrystallized with the GluA2-LBD,*28−33* we clearly observed a close proximity of two modulators in two binding sites at the dimer interface. Thus, we hypothesized that it should be possible to design dimeric compounds linked together via the 6-position of the respective BTD monomers (Figure 2), providing new ligands with a significant enhancement of potency on AMPARs. This assumption was reinforced by our recent work on 7-phenoxy-substituted BTDs.[26] Indeed, we demonstrated that these compounds occupied the C subsite with their BTD moiety, spanning the A subsite and pointing the methoxy substituent toward the B′ subsite where water-mediated interactions took place between receptor subunits.[26] Therefore, we reasoned that it could be possible to design rather large molecules that would interact on both sites of the

Published in : Journal of Medicinal Chemistry (2018), vol. 61, issue 12, pp. 5279-5291
doi.org/10.1021/acs.jmedchem.8b00250
Status : Postprint (Author's version)

GluA2-LBD dimer interface. Starting from such hypothesis, we elaborated our work with an initial molecular modeling approach (docking studies) to predict what would be the most potent dimeric modulator candidates. These molecules were synthesized, pharmacologically evaluated, and then compared to their respective monomers in order to demonstrate a gain of activity on the AMPAR by the design of dimeric compounds, and finally cocrystallized with the $GluA2_o$-LBD as an ultimate proof of concept.

Results and discussion

Dimeric compounds design based on docking studies.

In order to prioritize the synthesis of novel compounds, we decided to dock potential dimeric combinations and to compare the obtained results with the position of the two isolated monomers (compound 6) in the crystal structure (PDB code 4N07).[29] According to the distance between the two monomers in the crystal structure, we estimated that an ethylene or a propylene spacer would be appropriate to generate dimeric structures. The anchoring points for the linker were set to the 6,6-, 7,7-, or 6,7-position. We also considered amide or methylamine linkers instead of the alkyl-linking group. The alkyl substituent at the 4-position was chosen in accordance with previously established structure−activity relationships (SAR) (a methyl radical as the smallest alkyl group and a cyclopropyl radical known to confer the highest potency in the BTD series of AMPApams). Finally, we evaluated the possibility to simplify the structure by replacing one of the BTD monomers by a simpler benzenesulfonamide group. On this ground, a total of 10 potential dimeric compounds were designed and docked using the automated GOLD 5.3.0 program, while the binding energy and interactions were obtained using Discovery Studio 4.0. The docking solutions were ranked and analyzed according to the occurrence of compounds in each cluster, the ChemPLP score, the calculated binding energy, and the superimposition with compound 6 in the crystal structure (see Supporting Information for details on the interactions between the docking pose and the target).

From the results of this docking study, it seems that an ethylene linker would be more favorable compared to a propylene, an amide or a methylamine linker, and that the anchoring point should preferably be the 6,6-position (Table 1). While a propylene linker associated with a N-methyl moiety gives a promising calculated binding energy, its superimposition with the monomer in the crystal structure was found to be less satisfactory (see dimeric compounds C and D in the Supporting Information). The simplification of the dimeric structure through the replacement of one BTD monomer with a benzenesulfonamide group led to a marked decrease of estimated binding energy. Taken together, the results of this analysis highlighted the potential interest of the dimeric compounds A (16) and B (22) with an ethylene bridge between the two 6-positions of the respective BTD scaffolds for potent AMPAR positive allosteric modulation.

Synthesis of the target compounds.

The synthetic pathways giving access to the two desired dimeric molecules 16 and 22 are shown in Schemes 1 and 2. It should be noted that the change of the nature of the substituent on the nitrogen atom at the 4-position led to a complete change in the synthetic pathway. For the 4-methyl-substituted dimeric compound 16, a classical convergent method was used, and we first realized the synthesis of the monomeric BTD intermediate 14 according to previously described protocols[29] except the use of a Suzuki's coupling reaction for vinylation at the 6-position.

Published in : Journal of Medicinal Chemistry (2018), vol. 61, issue 12, pp. 5279-5291
doi.org/10.1021/acs.jmedchem.8b00250
Status : Postprint (Author's version)

Scheme 1. Synthetic Pathway Leading to the 4-Methyl-Substituted 3,4-Dihydro-2H-1,2,4-benzothiadiazine 1,1-Dioxide Dimeric Compound 16[a]

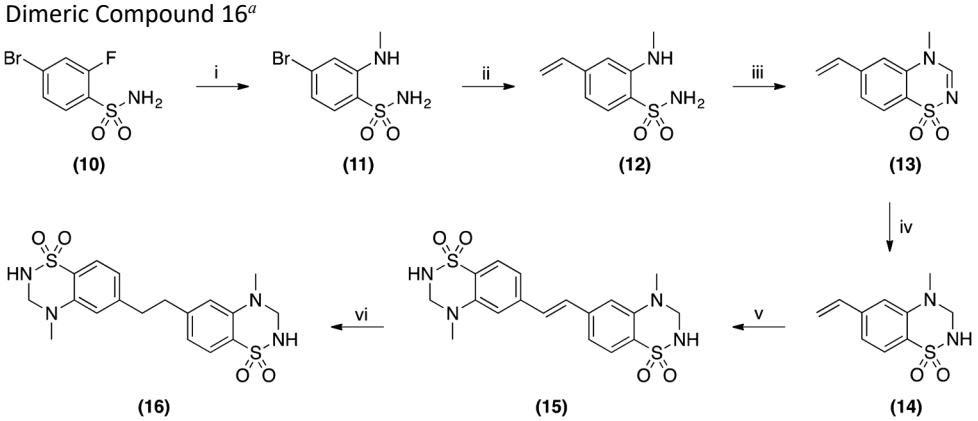

[a]i: methylamine, μw, yield: 96%; ii: $KBF_3CH{=}CH_2$, $Pd(OAc)_2$, KF, μw, yield: 33%; iii: triethyl orthoformate, 130°C, yield: 81%; iv: $NaBH_4$, 2-propanol, yield: 61%; v: Hoveyda-Grubbs II catalysts, CH_2Cl_2, yield: 65%; vi: Pd/C 10%, H_2, 12 bars, yield: 25%.

Scheme 2. Synthetic Pathway Leading to the 4-Cyclopropyl-Substituted 3,4-Dihydro-2H-1,2,4-benzothiadiazine 1,1-Dioxide Dimeric Compound 22[a]

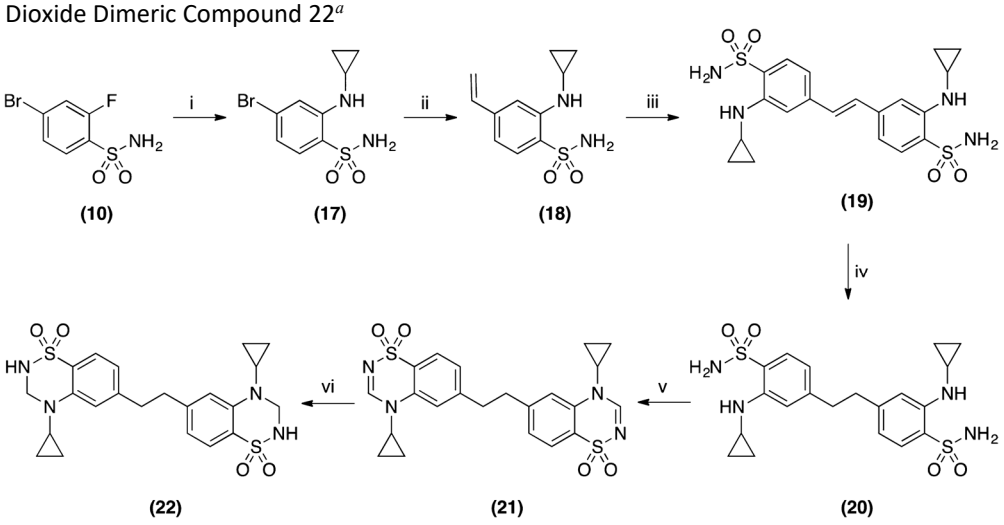

[a]i: cyclopropylamine, 1,4-dioxane, μw, yield: 75%; ii: $KBF_3CH{=}CH_2$, $Pd(OAc)_2$, KF, μw, yield: 86%; iii: Hoveyda-Grubbs II catalysts, CH_2Cl_2, yield: 89%; iv: Pd/C 10%, H_2, 12 bars, yield: 90%; v: triethyl orthoformate, 130°C; yield: 87% vi: $NaBH_4$, 2-propanol, yield: 82%.

Finally, the 6vinyl-substituted monomer 14 was coupled through a Grubbs' metathesis for dimerization to obtain the dimeric intermediate 15, which gave access to the final compound 16 after hydrogenation (Scheme 1). For the 4-cyclopropyl-substituted dimeric molecule 22, the same synthetic pathway was investigated, but the classical ring formation with triethyl orthoformate on intermediate 18 led to uncharacterized byproducts. A second pathway was developed in which the dimerization took place before the ring closure reaction, and then the benzothiadiazine dioxide cycle was obtained on both sides of the dimeric molecule according to classical protocols (Scheme 2).

Concerning the monomeric compounds selected for comparison purposes in this work, the BTDs 34 and 35 devoid of a substituent at the 6-position were synthesized as previously described.[29,34] The corresponding 6-methyl-substituted BTDs 28 and 33 were obtained using a slightly modified pathway compared to their corresponding unsubstituted analogs at the 6-position (Schemes 3 and 4).

Published in : Journal of Medicinal Chemistry (2018), vol. 61, issue 12, pp. 5279-5291
doi.org/10.1021/acs.jmedchem.8b00250
Status : Postprint (Author's version)

Scheme 3. Synthetic Pathway Leading to the 4,6-DimethylSubstituted BTD Monomer 28[a]

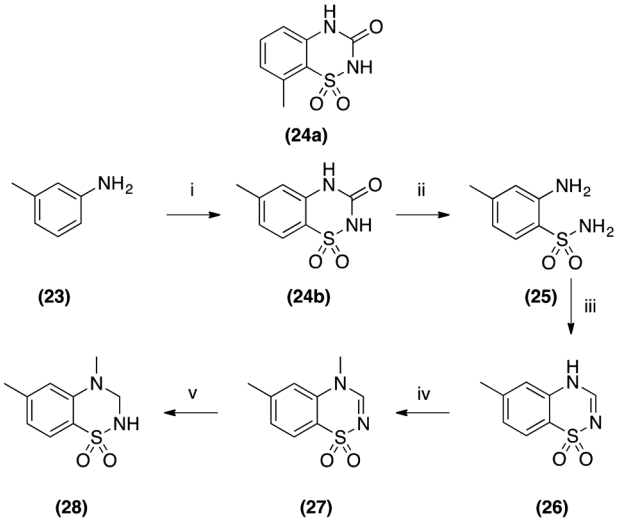

[a]i: 1: $ClSO_2NCO$, CH_3NO_2; 2: $AlCl_3$; ii H_2SO_4 50%, Δ, yield from 23: 19%; iii: triethyl orthoformate, 130°C, yield: 76%; iv: CH_3I, K_2CO_3, CH_3CN, yield: 75%; v: $NaBH_4$, 2-propanol, yield: 75%.

Starting from m-toluidine (23), the ring closure reaction was performed with chlorosulfonyl isocyanate in the classical experimental conditions described by Girard et al.[35] The reaction provided a mixture of two geometric isomers (24a and 24b) (Scheme 3). The mixture was engaged in the next step of hydrolysis by means of concentrated sulfuric acid in water (50% w/v). After 6 h at refluxing temperature, compound 24b was predominantly converted into the corresponding ring-opened aminobenzenesulfonamide 25, while compound 24a remained largely insoluble and unaffected in the acidic medium. After filtration, compound 25 was recovered in the filtrate, and then engaged in the next usual steps[34] up to the target compound 28 (Scheme 3).

For the synthesis of 33, starting compound 2-fluoro-4-methylaniline (29) was converted into the corresponding 2-fluoro-4-methylbenzenesulfonamide 30 after diazotization according to the Meerwein conditions.[36] The *o*-fluorobenzenesulfonamide 30 was then converted to the target compound 33 according to a multistep sequence previously described for 4-cyclopropyl-substituted 3,4-dihydro-2*H*-1,2,4-benzothiadiazine 1,1-dioxides (Scheme 4).[29]

Scheme 4. Synthetic Pathway Leading to the 4-Cyclopropyl-6-methyl-Substituted BTD Monomer 33[a]

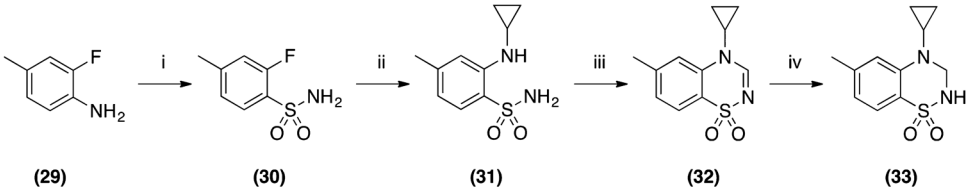

[a]i: 1: HNO_2, −5°C; 2: SO_2, Cu_2Cl_2, HOAc; 3: NH_3, yield: 37%; ii: cyclopropylamine, 1,4-dioxane, Δ, yield: 35%; iii: triethyl orthoformate, 130°C, yield: 35%; iv: $NaBH_4$, 2-propanol, yield: 75%.

Dramatic increase of the potency of AMPApams by the dimeric design.

The evaluation of the two dimeric molecules 16 and 22 and their constitutive monomers 28, 33, 34, and 35 as AMPApams was achieved with a fluorescencebased calcium assay as previously described.[26] HEK293 cells stably expressing $GluA2_o$(*Q*) were loaded with the calciumsensitive fluorescent probe Fluo-4-AM. The cells were incubated with the modulators at different concentrations and stimulated with L-glutamate (1 mM).[37]

Published in : Journal of Medicinal Chemistry (2018), vol. 61, issue 12, pp. 5279-5291
doi.org/10.1021/acs.jmedchem.8b00250
Status : Postprint (Author's version)

The intensity of fluorescence emission is positively correlated to the cytoplasmic concentration of calcium ions and hence can be used as a surrogate measure to estimate the calcium influx from extracellular medium through the open AMPAR channel. Therefore, this assay is suitable to determine the potentiating activity of the compounds on the L-glutamate-induced AMPAR opening. From the data obtained, the pEC_{50} values (negative logarithm of the modulator concentration responsible for 50% of the maximum effect) were calculated for the six selected molecules and compared with the pEC_{50} values obtained in the same conditions for the reference compounds 6 and 8 (Table 2; Figure 3).

As expected from previous SAR studies on BTD-type AMPApams,[20,25] the cyclopropyl substituent at the 4-position was always found to be the optimal (cyclo)alkyl chain with a gain of potency compared to the corresponding 4-methylsubstituted compounds of at least one log unit (compare 35 versus 34; 33 versus 28; 22 versus 16). Introduction of a methyl group at the 6-position in both series giving compounds 28 and 33 was responsible for a marked decrease of potency on AMPARs compared to the unsubstituted compounds 34 and 35 (compare 28 versus 34 and 33 versus 35) supporting the view that the absence of a substituent at this position should be preferred. On the contrary, with the dimeric compounds bearing an alkyl link at this key position, a substantial improvement of activity on AMPARs, up to more than 10,000 times (4 log units) compared to their corresponding monomers, was observed (compare 16 versus 34; 22 versus 35). This major enhancement led to the identification of one of the most potent AMPApams (compound 22) ever described with an EC_{50} value of 1.4 nM (pEC_{50} value of −8.90).

We recently demonstrated that the Hill coefficient (HC), which is sometimes improperly referred to as the "slope" of the sigmoidal curve,[38] of the concentration−response curves obtained in our functional assay was a good surrogate to estimate the binding stoichiometry of AMPApams.[26] Therefore, calculation of the HC has been included in Table 2. It was noticed that compounds 16 and 22 were characterized by a HC closer to unity, a profile that we previously observed for compound 8.[26] Such observations strongly suggest that the dimeric compounds have a different binding stoichiometry compared to their monomeric counterparts 28 and 33. These data are consistent with the nature of these dimeric compounds establishing a bridge between two AMPAR subunits, forming a single binding pocket at this interface.

The observation that the interaction of 7-phenoxysubstituted BTDs with two distant AMPAR subunits led to a drastic enhancement of the activity[26] seems to be confirmed here with the dimeric compounds. To our knowledge, the BTD-type AMPApam family shows an effect either on the deactivation or the desensitization process.[2] With the dimeric modulators we observe a "staple effect", or at least a bridge effect, in which the dimeric compound acts by "sticking" the two LBD subunits together, leading to a locked position of the 2-fold symmetric GluA2 dimer and thus most probably inhibiting completely the desensitization phenomenon. This hypothesis is strengthened by studies on iGluRs involving rigid bridging through cysteine−cysteine interaction where the linking of the two different parts of the LBD with a similar bridge significantly affected desensitization.[39−41]

Published in : Journal of Medicinal Chemistry (2018), vol. 61, issue 12, pp. 5279-5291
doi.org/10.1021/acs.jmedchem.8b00250
Status : Postprint (Author's version)

Table 2. Potentiating Effects of the 3,4-Dihydro-2H-1,2,4benzothiadiazine 1,1-Dioxide Dimeric Molecules 16 and 22 Compared to the Corresponding Monomers 28, 33, 34, and 35 on the Calcium Flux Induced by 1 mM L-Glutamate on HEK293 Cells Stably Expressing the GluA2$_o$(Q) Subunit and Their Respective Hill Coefficients

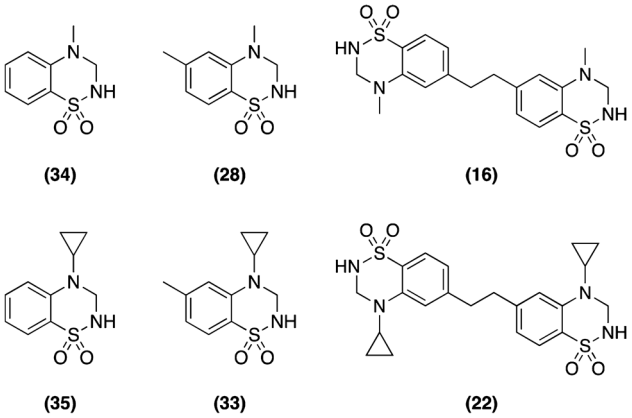

compounds	pEC$_{50}$[a] [mean ± SEM (n)]	corresponding EC$_{50}$[b] (μM)	Hill coefficient[c] [mean ± SEM (n)]
34	3.75 ± 0.02 (3)	176.3	2.8 ± 0.4 (3)
28	3.39 ± 0.02 (3)	403.3	2.8 ± 0.4 (3)
16	7.87 ± 0.04 (3)	0.0134	1.2 ± 0.1 (3)
35	5.04 ± 0.02 (3)	9.06	2.2 ± 0.2 (3)
33	4.31 ± 0.03 (3)	48.2	2.2 ± 0.3 (3)
22	8.90 ± 0.05 (3)	0.0014	1.7 ± 0.2 (3)
6	6.090 ± 0.004 (3)[d]	0.81[d]	3.5 ± 0.1 (3)[d]
8	8.70 ± 0.05 (6)[d]	0.002[d]	1.4 ± 0.2 (6)[d]

[a]pEC$_{50}$: negative logarithm of the AMPApam concentration responsible for 50% of the maximal effect (mean ± SEM (*n*)). [b]EC$_{50}$: mean concentration responsible for 50% of the maximal effect, in μM. [c]The Hill coefficient is given as the mean value ± SEM (n). [d]Results form Goffin et al.[26]

Cocrystallization of dimeric compound 16 with GluA2$_o$-LBD shows 1:2 stoichiometry.

To establish the binding mode of 16 at AMPARs, we crystallized 16 in complex with GluA2$_o$-LBD and L-glutamate. Diffraction data were collected to a high resolution of 1.4 Å (Table 3). The complex crystallized with two GluA2$_o$-LBD molecules in the crystal asymmetric unit, forming a dimer (Figure 4A). Unambiguous electron density was observed for L-glutamate in both orthosteric binding sites and for one molecule of 16 at the dimer interface (Figure 4B). In the presence of 16, L-glutamate induces a domain closure of 20.7° (chain A) and 21.7° (chain B) relative to the apo structure of GluA2$_o$-LBD (PDB code 1FTO, chain A). These domain closures are similar to those observed with L-glutamate with no modulator bound.[42]

Compound 16 binds at GluA2 in a low energy conformation (2.8 kJ/mol above the global energy minimum). Therefore, introducing an ethylene bridge in 16 only gives rise to a minor conformational penalty. For the dimeric modulator 16, the potency at GluA2 was increased ~30 000 and ~13 000 times, respectively, compared to its monomeric parent compound 28 (6-methyl) and the monomeric compound containing a 6hydrogen (34) (Table 1). Similarly, compound 22 was superior to its monomeric parent compounds 33 (~34 000) and 35 containing 6-hydrogen (~6 000). The increase in potencies corresponds to a more favorable energy of 22−26 kJ/mol. It has previously been shown that the potency of a bivalent modulator was greater than the sum of its fragments.[27] This could be due to a decreased loss of rotational and translational entropy (from freezing of the overall molecular motion) in the dimeric compound resulting from joining the fragments compared to the binding of two individual components of the monomer.

Published in : Journal of Medicinal Chemistry (2018), vol. 61, issue 12, pp. 5279-5291
doi.org/10.1021/acs.jmedchem.8b00250
Status : Postprint (Author's version)

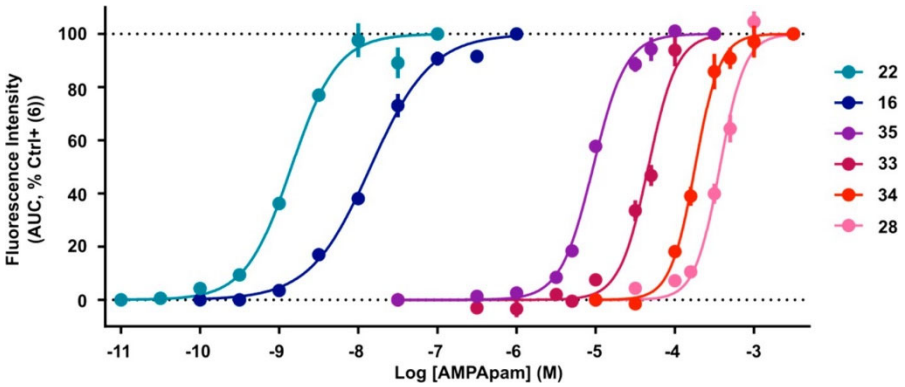

Figure 3. Concentration−response curves obtained in a fluorescence-based calcium assay in GluA2$_o$(Q)-transfected HEK293 cells. Compounds 16 and 22 show a marked increase in potency compared to their corresponding monomers (28 and 34 for 16; 33 and 35 for 22).

Table 3. Crystal Data, Data Collection, and Refinement Statistics of GluA2$_o$-LBD in Complex with L-Glutamate and 16

Crystal Data	
PDB-code	6FAZ
beamline	BioMAX, MAX-IV
space group	$P2_12_12$
unit cell dimensions (Å)	97.21, 121.46, 47.16
molecules in a.u.[a]	2
Data Collection and Processing	
resolution (Å)	47.16−1.40 (1.47−1.40)[b]
unique reflections	110,730 (15,969)
average multiplicity	13.3 (13.4)
completeness (%)	100 (100)
wilson *B*-factor (Å^2)	16.6
R_{merge} (%)[c]	5.5 (64.3)
$I/\sigma I$	7.2 (1.2)
Refinement	
numbers of	
amino-acid residues (chain A/chain B)	263/260
compound **16**	1
L-glutamate/sulfate/PEG/glycerol/chloride/ acetate/ethylene glycol/water	2/5/2/5/5/3/2/677
R_{work}[d] (%)/R_{free}[e] (%)	13.6/16.8
average B-values (Å^2) for	
amino acid residues (chain A/chain B)	22.6/26.4
compound **16**	26.5
L-glutamate/sulfate/PEG/glycerol/chloride/ acetate/ethylene glycol/water	15.6/40.1/43.9/49.2/55.7/ 38.2/37.8/33.3
RMS deviation bonds length (Å)/angles (deg)	0.007/0.98
Ramachandran outliers/favored (%)[f]	0/99.1
rotamer ouliers (%)/Cβ outliers (%)/clash score	0.8/0/2.54

[a]a.u.: asymmetric unit of the crystal. [b]Values in parentheses correspond to the outermost resolution shell. [c]$R_{merge} = \Sigma_{hkl}\Sigma_i|I_{i,hkl} - I_{hkl}|/\Sigma_{hkl}\Sigma_i|I_{hkl}|$, $I_{i,hkl}$ is the intensity of an individual measurement of the flection with Miller indices *hkl* and I_{hkl} is the intensity from multiple observations. [d]$R_{work} = \Sigma_{hkl}(||F_{o,hkl}| - |F_{c,hkl}||)/|F_{o,hkl}|$, where $|F_{o,hkl}|$ and $|F_{r,hkl}|$ are the observed and calculated structure factor amplitudes, respectively. [e]R_{free} is equivalent to R_{work}, but calculated with 5% of the reflections omitted from the refinement process. [f]The Ramachandran plot was calculated according to MolProbity.[56]

However, other aspects related to enthalpy might also be involved such as decreased rate of dissociation of the dimer. The 6-hydrogen containing compounds 34 and 35 have a greater potency than 6-methyl compounds 28 and 33 (∼2 and 5 times, respectively). This is in agreement with that 34 and 35 can bind in

Published in : Journal of Medicinal Chemistry (2018), vol. 61, issue 12, pp. 5279-5291
doi.org/10.1021/acs.jmedchem.8b00250
Status : Postprint (Author's version)

a similar manner in GluA2 as 16, whereas a different binding mode is required for 28 and 33 to avoid clash between the two methyl groups.

Compound 16 binds to the allosteric binding site in the same region as other BTD modulators. The binding mode of the dimeric modulator 16 is similar to that of the monomeric modulator 6 (Figure 4C). However, a slight displacement of the BTD ring systems of ~0.5 Å was observed. Previously, it was shown that introduction of a cyclopropyl group at the 4-N nitrogen in the monomeric modulator (6) led to 10 times improved binding affinity compared to an ethyl group (5).[29] This is in agreement with what we observed in the present study, namely, a 10 times greater potency of 22 (with cyclopropyl) compared to 16 (with methyl) (Table 2). Compound 16 binds symmetrically in both the B/B' and C/C' subsites (Figure 4C).

Similarly to 16 and 22, compound 8 can be considered a dimeric modulator, but it is asymmetric. However, the 3-methoxyphenoxy substituent of 8 occupies a different space than the benzothiadiazine dioxide of 16, with the benzene ring positioned perpendicular to the backbone of Met517 and Ser518.[26]

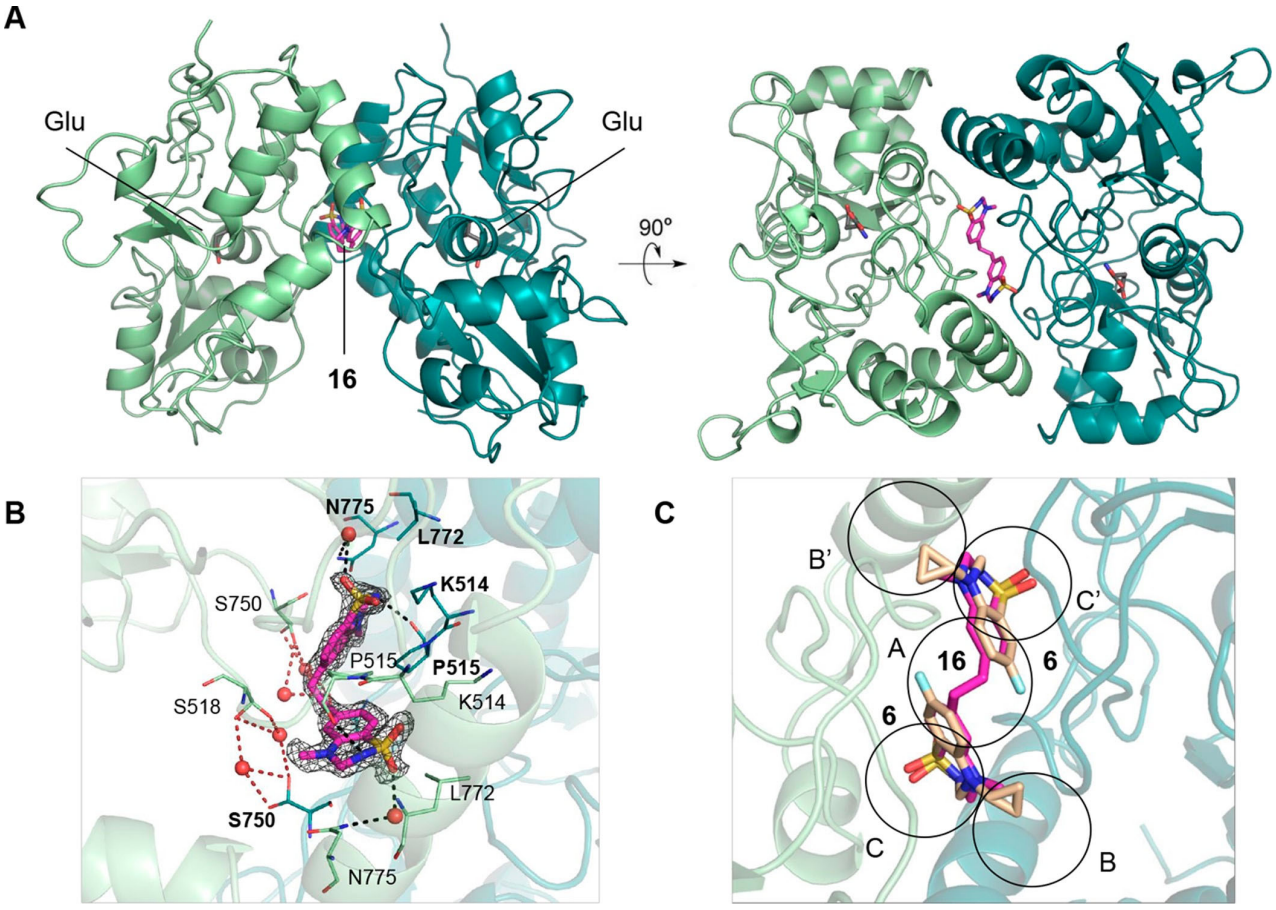

Figure 4. Structure of GluA2$_o$-LBD in complex with L-glutamate (Glu) and 16. (A) Left: side-view of the GluA2$_o$-LBD dimer (light green and dark green cartoon representation), showing that 16 (magenta sticks) binds in the lower part of the dimer interface. L-Glutamate is shown as gray sticks. Right: a 90° horizontally rotated view. (B) Zoom in on the modulator binding site, showing the $2F_o–F_c$ omit electron density map contoured at 1σ and carved at 1.2 Å around the modulator. Residues within 4 Å of 16 and protruding into the binding site are shown as lines. Polar interactions (up to 3.5 Å) of 16 with GluA2$_o$-LBD residues and water molecules (red spheres) are shown as stippled, black lines. In addition, water-mediated contacts between Ser518 and Ser750 are shown as red stippled lines. (C) Comparison of the binding mode of 16 and 6 (pdb code 4N07), showing that 16 and 6 (in beige sticks) occupy the same binding sites at the GluA2$_o$-LBD dimer interface. The circles indicate the different subsites. GluA2$_o$ chains belonging to the structure with 16 are shown as cartoon representation.

Published in : Journal of Medicinal Chemistry (2018), vol. 61, issue 12, pp. 5279-5291
doi.org/10.1021/acs.jmedchem.8b00250
Status : Postprint (Author's version)

The following residues are within 4 Å of 16: Lys514, Pro515, Phe516, Met517, Ser518, Ser750, Lys751, Gly752, Leu772, and Asn775 of both subunits comprising the GluA2$_o$-LBD dimer (numbering with signal peptide). Of these residues, Lys514, Pro515, Ser518, Ser750, Leu772, and Asn775 are protruding into the modulator binding site (Figure 4B). Notably, Ser518 and Ser750 are present in two side-chain conformations in both subunits of which one conformation of Ser518 in both subunits are lining the ethylene bridge of 16. Both conformations of Ser518 form water-mediated contacts to both conformations of Ser750 (Figure 4B). Compound 16 only forms two hydrogen bonds to the receptor subunits: a hydrogen bond is seen from both sulfonamide nitrogen atoms of 16 to the backbone oxygen atom of Pro515 in each subunit (Figure 4B). In addition, a water-mediated hydrogen bond is formed from an oxygen atom of each sulfonamide in 16 to the side chain of Asn775. Thus, the monomeric parts of 16 make polar contacts to the receptor subunits in a symmetrical manner.

Conclusions

The aim of the present study was to develop dimeric compounds able to fit the allosteric binding sites located on both sides of the AMPAR dimer interface. The design of such molecules was motivated by the putative gain of activity resulting from a double occupancy of the binding site. Previous X-ray data obtained with "monomeric" BTD-type AMPApams clearly highlighted the close proximity of two molecules of such modulator on two close receptor subunits and that it could be possible to design dimeric molecules interacting with both sides of the LBD dimer interface.

Molecular modeling was used to perform the virtual docking of a series of large dimeric molecules in the double-sided allosteric pocket. The best fits were obtained with dimeric compounds linked together by an ethylene bridge between their respective 6-positions. It should be noticed that there was a little difference in the predicted binding affinities between compounds differing by the nature of the substituent (methyl or cyclopropyl) introduced at the 4-position of the two BTD scaffolds.

According to these data, two dimeric molecules, compounds 16 and 22, were selected for chemical synthesis. This was done following two different synthetic pathways. For the 4-methylsubstituted compound 16, a convergent pathway was developed in which the 1,2,4-benzothiadiazine 1,1-dioxide ring was first built and for which the cross-linkage took place in the last steps. For the 4-cyclopropyl-substituted compound 22, the crosslinking step was performed much earlier in the synthesis route, and the ring closure of the heterocycle was built in the final steps.

The pharmacological evaluation of the target compounds and their corresponding constitutive monomers was performed on HEK293 cells expressing the GluA2$_o$(Q) receptor, and the variations of cytoplasmic calcium content were followed with a fluorescent probe. The AMPApam activity of dimeric compound 22 was found to be approximately 10 times higher than dimeric compound 16, an observation that differs only slightly from the docking results. For the whole series of tested compounds, the cyclopropyl group was always found to be the best choice of alkyl substituent at the 4-position of the BTD ring. Interestingly, both dimeric molecules 16 and 22 showed about 10 000 times lower EC_{50} values than their corresponding unsubstituted BTD monomers (compounds 34 and 35). To the best of our knowledge, compound 22, with an EC_{50} value of 1.4 nM, may be considered as one of the most potent AMPApams ever described in the literature, expressing a potency in the same order of magnitude as the recently described compound 8.[26] Ultimately, the cocrystallization of dimeric compound 16 with GluA2$_o$-LBD clearly demonstrated that the

Published in : Journal of Medicinal Chemistry (2018), vol. 61, issue 12, pp. 5279-5291
doi.org/10.1021/acs.jmedchem.8b00250
Status : Postprint (Author's version)

two allosteric binding sites located at the LBD dimer interface were able to host the dimeric compound occupying the position of two separated monomers.

Experimental section

General procedures.

Melting points were determined on a Büchi Tottoli capillary apparatus and are uncorrected. The ^{1}H and ^{13}C NMR spectra were recorded on a Bruker Avance (500 MHz for ^{1}H; 125 MHz for ^{13}C) instrument using deuterated dimethyl sulfoxide (DMSO-d_6) as the solvent with tetramethylsilane (TMS) as an internal standard; chemical shifts are reported in δ values (ppm) relative to that of internal TMS. The abbreviations s = singlet, d = doublet, t = triplet, q = quadruplet, m = multiplet, dd = doublet of doublet, qd = quadruplet of doublet, dt = doublet of triplet, tt = triplet of triplet, and bs = broad singlet are used throughout. Elemental analyses (C, H, N, S) were realized on a Thermo Scientific Flash EA 1112 elemental analyzer and were within ±0.4% of the theoretical values for carbon, hydrogen, and nitrogen. This analytical method certified a purity of ≥95% for each tested compound. All reactions were routinely checked by TLC on silica gel Merck 60 F254.

4-Bromo-2-(methylamino)benzenesulfonamide (11).

4-Bromo-2-fluorobenzenesulfonamide (10) (4 g, 15.7 mmol) was dissolved in a 1:3 mixture of 1,4-dioxane and methylamine solution 40% in water (20 mL). The solution was heated in a microwave oven at 135 °C for 25 min. After cooling, the solvent was removed by distillation under reduced pressure. The pink solid was suspended in water, collected by filtration, and dried in a vacuum desiccator (yield: 96%). m.p., 171−173 °C; ^{1}H NMR (500 MHz, DMSO-d_6) δ 7.51 (d, J = 8.4 Hz, 1H, 6*H*), 7.38 (s, 2H, SO_2NH_2), 6.87 (d, J = 1.8 Hz, 1H, 3-*H*), 6.82 (dd, J =8.4 Hz/1.9 Hz, 1H, 5-*H*), 6.01 (q, J = 4.5 Hz, 1H, N*H*), 2.83 (d, J = 4.9 Hz, 3H, $NHCH_3$); ^{13}C NMR (125 MHz, DMSO-d_6) δ 146.7 (C1), 130.0 (C-6), 127.2 (C-4), 124.1 (C-2), 117.0 (C-5), 113.3 (C-3), 30.0 (NCH_3).

2-(Methylamino)-4-vinylbenzenesulfonamide (12).

To a solution of 4-bromo-2-(methylamino)benzenesulfonamide (11) (1.9 g, 7.17 mmol) in 1,4-dioxane (14 mL), potassium vinyltrifluoroborate (1.15 g, 8.6 mmol, 1.2 equiv) was added. Once the salt was completely solubilized, an aqueous solution of NaOH 10% (6.3 mL) was added, followed by $Pd(OAc)_2$ (4.3 mg, 0.27 mol %). This mixture was heated to reflux for 24 h. Once returned to room temperature, the crude black suspension was filtered. The aqueous filtrate was then extracted with ethyl acetate (3 × 25 mL). The organic layers were combined, washed with brine (15 mL), and dried over $MgSO_4$. The solvent was removed under reduced pressure, and the oily residue was recrystallized in a mixture of methanol/water 1:2 (yield: 33%). m.p., 128−131 °C; ^{1}H NMR (500 MHz, DMSO-d_6) δ 7.57 (d, J = 8.2 Hz, 1H, 6-*H*), 7.26 (s, 2H, SO_2NH_2), 6.80 (d, J = 8.3 Hz, 1H, 5-*H*), 6.76 (s, 1H, 3-*H*), 6.72 (dd, J = 17.7, 10.9 Hz, 1H, CH_2CH), 5.92 (d, J = 17.6 Hz, 1H, Z−CH_2CH), 5.87 (q, J = 4.9 Hz, 1H, $NHCH_3$), 5.35 (d, J = 10.9 Hz, 1H, E−CH_2CH), 2.86 (d, J = 4.9 Hz, 3H, NCH_3); ^{13}C NMR (125 MHz, DMSO-d_6) δ 145.9 (C-1), 141.8 (C-4), 136.4 (CH), 128.5 (C-6), 124.0 (C-2), 116.4 (CH_2), 111.9 (C-5), 109.0 (C-3), 29.6 (NCH_3).

Published in : Journal of Medicinal Chemistry (2018), vol. 61, issue 12, pp. 5279-5291
doi.org/10.1021/acs.jmedchem.8b00250
Status : Postprint (Author's version)

4-Methyl-6-vinyl-4h-1,2,4-benzothiadiazine 1,1-Dioxide (13).

2-(Methylamino)-4-vinylbenzenesulfonamide (12) (1.13 g, 5.3 mmol) was heated under stirring in triethyl othoformate (5 mL) at 135 °C for 4 h. The resulting suspension was cooled on an ice bath, and the solid product was collected by filtration, washed with ether, and dried (yield: 81%). m.p., >300 °C; ^{1}H NMR (500 MHz, DMSO-d_6) δ 8.08 (s, 1H, 3-*H*), 7.85 (d, *J* = 8.2 Hz, 1H, 8-*H*), 7.70 (dd, *J* = 8.3, 1.4 Hz, 1H, 7-*H*), 7.52 (d, *J* = 1.4 Hz, 1H, 5-*H*), 6.88 (dd, *J* = 17.7, 11.0 Hz, 1H CH_2CH), 6.14 (d, *J* = 17.6 Hz, 1H, Z−CH_2CH), 5.53 (d, *J* = 10.9 Hz, 1H, E−CH_2CH), 3.65 (s, 3H, NCH_3); ^{13}C NMR (125 MHz, DMSO-d_6) δ 151.3 (C-3), 141.7 (C-6), 136.2 (C-4a), 135.1 (CH), 124.4 (C-8), 123.9 (C-7), 121.6 (C-8a) 118.7 (CH_2), 114.3 (C-5), 38.2 (NCH_3).

4-Methyl-6-vinyl-3,4-dihydro-2h-1,2,4-benzothiadiazine 1,1-Dioxide (14).

4-Methyl-6-vinyl-4H-1,2,4-benzothiadiazine 1,1-dioxide (13) (0.4 g, 1.83 mmol) was stirred in suspension in isopropanol (10 mL) at 60 °C. $NaBH_4$ (0.2 g, 3 equiv) was added, and the mixture was stirred for 15 min. The solvent was removed by distillation under reduced pressure, the crude product was taken in water, and the suspension was adjusted to acidic pH by means of 6 N HCl. The aqueous suspension was then extracted with methylene chloride (3 × 30 mL). The combined organic layers were washed with brine and dried over $MgSO_4$. The filtrate was evaporated to dryness, and the resulting solid residue was suspended in water, collected by filtration, washed with water, and dried (yield: 61%). m.p., >300 °C; ^{1}H NMR (500 MHz, DMSO-d_6) δ 8.03 (t, *J* = 7.9 Hz, 1H, N*H*), 7.49 (d, *J* = 8.1 Hz, 1H, 8-*H*), 6.95 (d, *J* = 8.1 Hz, 1H, 7-*H*), 6.88 (d, *J* = 1.4 Hz, 1H, 5-*H*), 6.72 (dd, *J* = 17.6, 10.9 Hz, 1H, CH_2CH), 5.95 (dd, *J* = 17.6, 0.8 Hz, 1H, Z−CH_2CH), 5.38 (d, J = 11.0 Hz, 1H, E−CH_2CH), 4.65 (d, *J* = 8.1 Hz, 2H, CH_2), 2.97 (s, 3H, NCH_3); ^{13}C NMR (125 MHz, DMSO-d_6) δ 144.4 (C-6), 141.6 (C-4a), 136.2 (CH_2CH), 124.4 (C8), 122.0 (C-8a), 116.5 (CH_2CH), 113.6 (C-7), 111.7 (C-5), 62.2 (C3), 35.9 (NCH_3).

(E)-6,6′-(Ethene-1,2-diyl)bis(4-methyl-3,4-dihydro-2h-1,2,4-benzothiadiazine 1,1-dioxide) (15).

4-Methyl-6-vinyl-3,4-dihydro-2H1,2,4-benzothiadiazine 1,1-dioxide (14) (0.2 g, 0.89 mmol) was solubilized in methylene chloride (3 mL) and supplemented with Hoveyda-Grubbs II catalyst (0.01 mol %) under nitrogen, and the mixture was heated to reflux. Every 30 min, the nitrogen was fluxed and replaced with fresh volume. After 4 h, the reaction mixture was cooled to room temperature, and the solid was collected by filtration, washed with ether, and dried (yield: 65%). m.p., 331 °C (decomposition); ^{1}H NMR (500 MHz, DMSO-d_6) δ 8.06 (t, *J* = 7.9 Hz, 1H, N*H*), 7.54 (d, *J* = 8.1 Hz, 1H, 8-*H*), 7.37 (s, 1H, C*H*), 7.10 (dd, *J* = 8.2, 1.6 Hz, 1H, 7-*H*), 7.05 (d, *J* = 1.5 Hz, 1H, 5-*H*), 4.68 (d, *J* = 7.6 Hz, 2H, CH_2), 3.01 (s, 3H, NCH_3); ^{13}C NMR (125 MHz, DMSO-d_6) δ 144.3 (C-6), 141.2 (C-4a), 130.0 (CH linker), 124.5 (C8), 121.8 (C-8a), 114.3 (C-7), 112.2 (C-5), 62.3 (C-3), 36.2 (NCH_3).

6,6′-(Ethane-1,2-diyl)bis(4-methyl-3,4-dihydro-2h-1,2,4-benzothiadiazine 1,1-dioxide) (16).

(E)-6,6′-(Ethene-1,2-diyl)bis(4-methyl3,4-dihydro-2H-1,2,4-benzothiadiazine 1,1-dioxide) (15) (0.13 g, 0.31 mmol) was dissolved in DMF (5 mL) and was supplemented with 10% palladium on charcoal (13 mg). The resulting suspension was placed under 12 bar of H_2 for 1 h. The solvent was removed by distillation under reduced pressure, and the residue was recrystallized in methanol, collected by filtration, and dried (yield: 25%). m.p., 313 °C (decomposition); ^{1}H NMR (500 MHz, DMSO-d_6) δ 7.91 (s, 1H, N*H*), 7.42 (d, *J* = 7.4 Hz, 1H, 8-*H*), 6.71 (s, 1H, 5-*H*), 6.70 (dd, *J* = 7.1 Hz/1.2 Hz, 1H, 7-*H*), 4.62 (s, 2H, CH_2), 2.91 (s, 3H, NCH_3), 2.86 (s, 2H, CH_2 (linker)); ^{13}C NMR (125 MHz, DMSO-d_6) δ 146.9 (C-6), 144.0 (C-4a), 124.0 (C-8), 120.6 (C-8a), 116.8 (C-7), 113.4 (C-5), 62.4 (C-3), 36.7 (CH_2 linker), 36.2 (NCH_3). Anal. ($C_{18}H_{22}N_4O_4S_2$) calcd: N 13.26%, C 51.17%, H 5.25%, S 15.18%. Found: N 13.22%, C 51.29%, H 5.29%, S 14.71%.

Published in : Journal of Medicinal Chemistry (2018), vol. 61, issue 12, pp. 5279-5291
doi.org/10.1021/acs.jmedchem.8b00250
Status : Postprint (Author's version)

4-Bromo-2-(cyclopropylamino)benzenesulfonamide (17).

4-Bromo-2-fluorobenzenesulfonamide (10) (4.0 g, 15.7 mmol) was dissolved in a 1:1 mixture of 1,4-dioxane and cyclopropylamine (20 mL). The solution was heated in a microwave oven to 135 °C for 25 min. After cooling, the solvent was removed by distillation under reduced pressure. The solid residue was recrystallized from methanol/ water 1:2, collected by filtration, washed with water, and dried in a vacuum desiccator (yield: 75%). m.p., 201−204 °C; ^{1}H NMR (500 MHz, DMSO-d_6) δ 7.52 (d, J = 8.4 Hz, 1H, 6-*H*), 7.43 (bs, 2H, SO_2NH_2), 7.25 (d, J = 1.9 Hz, 1H, 3-*H*), 6.90 (dd, J = 8.4, 1.9 Hz, 1H, 5-*H*), 6.21 (d, J = 1.8 Hz, 1H, N*H*), 2.50 (m, 1H, C*H*$(CH_2)_2$), 0.87− 0.76 (m, 2H, CH(C*H*$_2$)$_2$), 0.56−0.49 (m, 2H, CH(C*H*$_2$)$_2$); ^{13}C NMR (125 MHz, DMSO-d_6) δ 146.6 (C-1), 129.9 (C-6), 126.8 (C-4), 124.4 (C-2), 118.0 (C-5), 114.9 (C-3), 24.2 (NCH_3), 7.1 ($CH(CH_2)_2$).

2-(Cyclopropylamino)-4-vinylbenzenesulfonamide (18).

The title compound was obtained according to the procedure described for compound 12 starting from compound 17 (yield: 86%). m.p., 155− 161 °C; ^{1}H NMR (500 MHz, DMSO-d_6) δ 7.61−7.51 (m, 1H, 6-*H*), 7.31 (s, 2H, SO_2NH_2), 7.15 (d, J = 1.6 Hz, 1H, 3-H), 6.87 (dd, J = 8.2, 1.6 Hz, 1H, 5-H), 6.74 (dd, J = 17.6, 10.9 Hz, 1H, C*H*CH_2), 6.11 (s, 1H, N*H*),, 5.90 (d, J = 1.7 Hz, 1H, Z-CHC*H*$_2$), 5.37 (d, J = 17.5 Hz, 1H, E-CHC*H*$_2$), 2.50 (m,, 1H, C*H*$(CH_2)_2$), 0.88−0.72 (m, 2H, CH(C*H*$_2$)$_2$), 0.57−0.43 (m, 2H, CH(C*H*$_2$)$_2$); ^{13}C NMR (125 MHz, DMSO-d_6) δ 146.0 (C-4), 141.0 (C-1), 136.3 ($CHCH_2$), 128.0 (C-6), 124.0 (C-2), 116.4 (CH_2), 113.0 (C-5), 110.7 (C-3), 24.5 ($CH(CH_2)_2$), 7.2 ($CH(CH_2)_2$).

(E)-4,4′-(Ethene-1,2-diyl)bis(2-(cyclopropylamino)benzenesulfonamide) (19).

The title compound was obtained according to the procedure described for compound 15 starting from compound 18 (yield: 89%). m.p., 247 °C (decomposition); ^{1}H NMR (500 MHz, DMSO-d_6) δ 7.61 (d, J = 8.3 Hz, 1H, 6-*H*), 7.37−7.28 (m, 3H, SO_2NH_2 and 3-*H*), 7.09 (dd, J = 8.4, 1.5 Hz, 1H, 5-*H*),6.16−6.11 (m, 1H, NH), 2.56 (tt, J = 6.4, 3.3 Hz, 1H, C*H*$(CH_2)_2$), 0.86 (m, J = 6.6, 3.3 Hz, 2H, CH(C*H*$_2$)$_2$), 0.55 (m, J = 4.4 Hz, 2H, CH(C*H*$_2$)$_2$); ^{13}C NMR (125 MHz, DMSO-d_6) δ 145.6 (C-4), 141.1 (C-1) 130.0 (C-6), 128.5 (CH linker), 124.1 (C-2), 113.3 (C-5), 111.6 (C-3), 24.6 (NCH), 7.4 ($CH(CH_2)_2$).

4,4′-(Ethane-1,2-diyl)bis(2-(cyclopropylamino)benzenesulfonamide) (20).

The title compound was obtained according to the procedure described for compound 16 starting from compound 19 (yield: 90%). m.p., 220−222 °C; ^{1}H NMR (500 MHz, DMSO-d_6) δ 7.50 (d, J = 8.1 Hz, 1H, 6-*H*), 7.23 (s, 2H, SO_2NH_2), 6.94 (d, J = 1.6 Hz, 1H, 3-*H*), 6.62 (dd, J = 8.1, 1.7 Hz, 1H, 5-*H*), 6.05 (d, J = 1.6 Hz, 1H, N*H*), 2.90 (s, 2H, C*H*$_2$), 2.43−2.37 (m, 1H, C*H*$(CH_2)_2$), 0.76 (dt, J = 6.6, 3.3 Hz, 2H, CH(C*H*$_2$)$_2$), 0.50−0.41 (m, 2H, CH(C*H*$_2$)$_2$); ^{13}C NMR (125 MHz, DMSO-d_6) δ 146.8 (C-4), 145.5 (C-1), 128.0 (C-6) 123.0 (C-2), 115.9 (C-5), 112.6 (C-3), 36.4 (CH_2 linker), 24.5 (NCH), 7.3 ($CH(CH_2)_2$).

6,6′-(Ethane-1,2-diyl)bis(4-cyclopropyl-4h-1,2,4-benzothiadiazine 1,1-dioxide) (21).

The title compound was obtained according to the procedure described for compound 13 starting from compound 20 (yield: 87%). m.p., 298 °C (decomposition); ^{1}H NMR (500 MHz, DMSO-d_6) δ 8.09 (s, 1H, 3-*H*), 7.81 (d, J = 8.1 Hz, 1H, 8-*H*), 7.53 (s, 1H, 5-*H*), 7.47 (d, J = 8.1 Hz, 1H, 7-H), 3.26 (m, J = 7.2, 3.9 Hz, 1H, C*H*$(CH_2)_2$), 3.15 (s, 2H, C*H*$_2$ linker), 1.09 (t, J = 6.6 Hz, 2H CH(C*H*$_2$)$_2$), 0.93−0.84 (m, 2H, CH(C*H*$_2$)$_2$); ^{13}C NMR (125 MHz, DMSO-d_6) δ 151.4 (C-3), 146.6 (C-6), 136.3 (C-4a), 127.2 (C-8), 124.1 (C-7), 120.3 (C-8a), 116.3 (C-5), 36.3 (CH_2 linker), 32.1 (NCH), 7.3 ($CH(CH_2)_2$).

Published in : Journal of Medicinal Chemistry (2018), vol. 61, issue 12, pp. 5279-5291
doi.org/10.1021/acs.jmedchem.8b00250
Status : Postprint (Author's version)

6,6′-(Ethane-1,2-diyl)bis(4-cyclopropyl-3,4-dihydro-2h-1,2,4-benzothiadiazine 1,1-dioxide) (22).

The title compound was obtained according to the procedure described for compound 14 starting from compound 21 suspended in isopropanol and adding DMF dropwise until the reactant was solubilized before the addition of $NaBH_4$ (yield: 82%). m.p., 290 °C (decomposition); ^{1}H NMR (500 MHz, DMSOd_6) δ 7.78 (t, J = 7.9 Hz, 1H, N*H*), 7.43 (d, J = 8.0 Hz, 1H, 8-*H*), 7.02 (d, J = 1.5 Hz, 1H, 5-*H*), 6.75 (dd, J = 8.1, 1.5 Hz, 1H, 7-*H*), 4.61 (d, J = 7.7 Hz, 2H, 3-*H*), 2.92 (s, 2H, CH_2 linker), 2.41 (m, 1H, CH(CH_2)$_2$), 0.90−0.84 (m, 2H, CH(CH_2)$_2$), 0.58 (m, 2H, CH(CH_2)$_2$); ^{13}C NMR (125 MHz, DMSO-d_6) δ 146.1 (C-6), 143.9 (C-4a), 124.2 (C-8), 121.2 (C-8a), 117.8 (C-7), 114.2 (C-5), 61.0 (C-3), 36.5 (CH_2 linker), 29.6 (NCH), 8.4 (CH(CH_2)$_2$). Anal. ($C_{22}H_{26}N_4O_4S_2$) calcd: N 11.80% C 55.68% H 5.52% S 13.51%. Found: N 11.77% C 55.88% H 5.67% S 13.05%.

2-Amino-4-methylbenzenesulfonamide (25).

A solution of mtoluidine (23) (10 g, 93.3 mmol) in nitromethane (40 mL) was added to a stirred, ice-cooled solution of chlorosulfonyl isocyanate (9 mL) in nitromethane (25 mL) during 5 min. This addition resulted in a suspension. Aluminum chloride (14.0 g, 105 mmol) was added at once, resulting in a clear solution. The reaction mixture was then refluxed for 30 min, cooled, and poured into ice−water. The precipitated solid was collected by filtration and washed with water. The precipitate was suspended in water and then extracted three times with ethyl acetate. The combined organic layers were dried over $MgSO_4$ and filtered. The filtrate was concentrated to dryness under reduced pressure. The residue was taken in water (100 mL), and the mixture was adjusted to pH 12 with NaOH 10% w/w in water, treated with charcoal, and filtered. The filtrate was then acidified by the addition of 12 N HCl, and the solid that precipitated was collected by filtration. This solid consisted in the mixture of the two isomers (24a and 24b). This solid was dispersed in 50% w/w sulfuric acid in water and refluxed during 6 h. After being cooled, the mixture was filtered and afforded a solid (mainly unchanged 24a) and a filtrate containing compound 25. After neutralizing the filtrate with NaOH 40% w/w in water, the solvent was evaporated under reduced pressure. The residue was suspended in hot ethanol (200 mL) and filtered. The resulting filtrate was concentrated to dryness under reduced pressure, and the residue of the title compound was recrystallized in methanol/water 1:2 (yield: 19%)/ m.p., 121−122 °C (lit. 124−126 °C[43]).

6-Methyl-4h-1,2,4-benzothiadiazine 1,1-dioxide (26).

The title compound was obtained according to the procedure described for compound 13 starting from compound 25 (yield: 76%). m.p., 186− 195 °C; ^{1}H NMR (DMSO-d_6, 500 MHz) δ 12.17 (s, 1H, N*H*), 7.94 (s, 1H, 3-*H*), 7.69 (d, 1H, 8-*H*), 7.58 (s, 1H, 5-*H*), 7.25 (d, 1H, 7-*H*), 2.39 (s, 3H, 6−CH_3); ^{13}C NMR (125 MHz, DMSO-d_6) δ 147.5 (C-3), 143.5 (C-6), 134.6 (C4a), 127.7 (C-8a), 123.6 (C-8), 120.1 (C-7), 117.0 (C-5), 21.1 (CH_3).

4,6-Dimethyl-4h-1,2,4-benzothiadiazine 1,1-dioxide (27).

The mixture of 6-methyl-4H-1,2,4-benzothiadiazine 1,1-dioxide (26) (1 g, 4.62 mmol), potassium carbonate (2 g), and methyl iodide (1.7 mL) in acetonitrile (30 mL) was heated at 60 °C for 3 h. The solvent was removed by distillation under reduced pressure, and the residue was suspended in water (40 mL). The resulting insoluble material was collected by filtration, washed with water, dried and recrystallized in ethyl acetate (yield: 75%). m.p., 269−272 °C; ^{1}H NMR (DMSO-d_6, 500 MHz) 8.04 (s, 1H, 3-H), 7.76 (d, 1H, 8-H), 7.37 (d, 1H, 7-H), 7.32 (s, 1H, 5-H), 3.59 (s, 3H, NCH_3), 2.44 (s, 3H, 6-CH_3); ^{13}C NMR (125 MHz, DMSO-d_6) δ 151.1 (C-3), 143.8 (C-6), 135.8 (C-4a), 127.7 (C-7), 124.0 (C-8), 120.2 (C-8a), 116.4 (C-5), 38.0 (NCH_3), 21.4 (6-CH_3).

Published in : Journal of Medicinal Chemistry (2018), vol. 61, issue 12, pp. 5279-5291
doi.org/10.1021/acs.jmedchem.8b00250
Status : Postprint (Author's version)

4,6-Dimethyl-3,4-dihydro-2h-1,2,4-benzothiadiazine 1,1-dioxide (28).

The title compound was obtained according to the procedure described for compound 14 starting from compound 27 (yield: 75%). m.p., 141−142 °C; ^{1}H NMR (DMSO-d_6, 500 MHz) δ 7.95 (t, 1H, NH) 7.40 (d, 1H, 8-H), 6.66 (s, 1H, 5-H), 6.62 (d, 1H, 7-H), 4.63 (d, 2H, 3-H_2), 2.92 (s, 3H, NCH_3), 2.29 (s, 3H, 6-CH_3); ^{13}C NMR (125 MHz, DMSO- d_6) δ 144.0 (C-6), 143.3 (C-4a), 124.0 (C-8), 120.3 (C8a), 117.3 (C-7), 113.8 (C-5), 62.3 (C-3), 36.1 (NCH_3), 21.6 (6CH_3). Anal. ($C_9H_{12}N_2O_2S$) calcd: N 13.20%, C 50.92%, H 5.70% S 15.10%. Found: N 13.14%, C 50.61%, H 5.50% S 15.53%.

2-Fluoro-4-methylbenzenesulfonamide (30).

A portion of glacial acetic acid (160 mL) was saturated for 30 min with gaseous sulfur dioxide. To the resulting solution, cooled on an ice bath, was added under stirring an aqueous solution of $CuCl_2$ (7 g in 20 mL) (suspension A). 2-Fluoro-4-methylaniline (29) (15 g, 87 mmol) was dissolved in a mixture of glacial acetic acid (160 mL) and 16 N HCl (40 mL). To the resulting solution, cooled in an ice−salt bath (−5 °C), was added dropwise under stirring an aqueous solution of $NaNO_2$ (8 g in 20 mL, 116 mmol). At the end of the addition, the resulting solution was slowly mixed with suspension A. After being stirred for 15 min, the suspension was poured onto ice (400 g). The resulting precipitate was collected by filtration, washed with water, and immediately dissolved in 1,4-dioxane (150 mL). The solution obtained was added gradually, under stirring, to a concentrated ammonium hydroxide solution (300 mL) previously cooled on an ice bath. After the resulting solution was stirred for 30 min, the organic solvent and part of the ammonia were removed by evaporation under reduced pressure. The aqueous solution/suspension obtained was adjusted to neutral pH by adding 6 N HCl. The precipitate formed was collected by filtration, washed with water, and dried (yield: 37%). m.p., 136− 137 °C; ^{1}H NMR (500 MHz, DMSO-d_6) δ 7.66 (t, J = 7.9 Hz, 1H, 8*H*), 7.59 (d, J = 4.7 Hz, 2H, SO_2NH_2), 7.26 (d, J = 11.3 Hz, 1H, 7-*H*), 7.17 (t, J = 6.4 Hz, 1H, 3-*H*), 2.38 (d, J = 4.0 Hz, 3H, CH_3); ^{13}C NMR (125 MHz, DMSO-d_6) δ 158.9−156.9 (d, J = 252.3 Hz, C-2), 145.5 (C-1), 128.8−128.7 (d, J = 14.4 Hz, C-6), 128.1 (C-4), 124.9 (C-5), 117.3−117.1 (d, 20.8 Hz, C-3), 20.8 (CH_3).

2-(Cyclopropylamino)-4-methylbenzenesulfonamide (31).

2-Fluoro-4-methylbenzenesulfonamide (30) (5 g, 21 mmol) was introduced into a hermetically closed vessel containing a mixture of 1,4-dioxane (70 mL) and cyclopropylamine (3.5 mL, 50 mmol). The closed vessel was placed in an oven at 100 °C for 240 h. After this time period, the solvent and the reagent were removed by distillation under reduced pressure. The residue was taken up in methanol (20 mL), and the insoluble material, which contained the title product, was collected by filtration, washed with methanol, and dried. This compound was used in the next step without further purification (yield: 35%). ^{1}H NMR (500 MHz, DMSO-d_6) δ 7.48 (d, J = 7.9 Hz, 1H, 6-*H*), 7.23 (s, 2H, SO_2NH_2), 6.94 (s, 1H, 3-*H*), 6.58−6.49 (m, 1H, 5-*H*), 6.06 (s, 1H, N*H*), 2.45 (dp, J = 9.7, 3.7, 3.2 Hz, 1H, C*H*(CH_2)$_2$), 2.29 (s, 3H, CH_3), 0.85−0.71 (m, 2H, CH(CH_2)$_2$), 0.50 (p, J = 4.3 Hz, 2H, CH(CH_2)$_2$); ^{13}C NMR (125 MHz, DMSO-d_6) δ 145.4 (C-4), 143.2 (C-1), 128.1 (C-6), 122.6 (C-2), 116.4 (C-5), 113.0 (C-3), 24.5 (CH(CH_2)$_2$), 21.5 (CH_3), 7.3 (CH(CH_2)$_2$).

4-Cyclopropyl-6-methyl-4h-1,2,4-benzothiadiazine 1,1-dioxide (32).

The title compound was obtained according to the procedure described for compound 13 starting from compound 31 (yield: 35%). m.p., 224−226 °C; ^{1}H NMR (500 MHz, DMSO-d_6) δ 8.12 (s, 1H, 3-*H*), 7.77 (d, J = 7.9 Hz, 1H, 8-*H*), 7.64 (s, 1H, 5-*H*), 7.39 (d, J = 8.4 Hz, 1H, 7-*H*), 3,34 (bs with water, 1H, NC*H*), 2.48 (s, 3H, CH_3), 1.30−1.08 (m, 2H, CH(CH_2)$_2$), 1.00 (dt, J = 6.9, 4.9 Hz, 2H, CH(CH_2)$_2$); ^{13}C NMR (125 MHz, DMSO-d_6) δ

Published in : Journal of Medicinal Chemistry (2018), vol. 61, issue 12, pp. 5279-5291
doi.org/10.1021/acs.jmedchem.8b00250
Status : Postprint (Author's version)

151.4 (C-3), 143.7 (C-6), 136.5 (C-4a), 127.6 (C-7), 124.0 (C-8), 119.8 (C-8a), 116.5 (C-5), 32.1 (CH_3), 21.6 (NCH), 7.3 ($CH(CH_2)_2$).

4-Cyclopropyl-6-methyl-3,4-dihydro-2h-1,2,4-benzothiadiazine 1,1-dioxide (33).

The title compound was obtained according to the procedure described for compound 14 starting from compound 32 (yield: 75%). m.p., 157−158 °C; ^{1}H NMR (500 MHz, DMSO-d_6) δ 7.81 (s, 1H, N*H*), 7.45−7.38 (d, *J* = 8.0 Hz, 1H, 8-*H*), 7.08 (s, 1H, 5-*H*), 6.70 (d, *J* = 8.0 Hz, 1H, 7-*H*), 4.63 (d, *J* = 4.9 Hz, 2H, CH_2), 2.32 (d, *J* = 5.1 Hz, 3H, CH_3), 0.92 (qd, *J* = 6.5, 4.2 Hz, 2H, CH(CH_2)$_2$), 0.65 (q, *J* = 4.1, 2.8 Hz, 2H, CH(CH_2)$_2$); ^{13}C NMR (125 MHz, DMSO-d_6) δ 144.1 (C-6), 142.9 (C-4a), 124.2 (C-8), 120.8 (C-8a), 118.3 (C-7), 114.5 (C-5), 61.1 (C-3), 29.6 (CH_3), 21.7 (NCH), 8.4(CH(CH_2)$_2$). Anal. ($C_{11}H_{14}N_2O_2S$) cald: N 11.76%, C 55.44%, H 5.92%, S 13.45%. Found: N 12.10%, C 55.78%, H 5.99%, S 13.60%.

Fluorescent-based calcium assay on GluA2$_o$(Q) cells.

The pharmacological evaluation of the target molecules was performed as described previously.[26] Briefly, HEK293 cells stably expressing AMPA channel GluA2$_o$(Q) were routinely grown in Dulbecco's modified Eagle's medium (DMEM) containing 10% fetal bovine serum (FBS), 1% penicillin and streptomycin (5000 U/mL), 1% L-glutamine (200 mM), and Geneticin (G418−600 mg/mL). The measurement of the fluorescence intensity was carried out using fluorescent microplate reader Fluoroskan Ascent FT equipped with two dispensers (Thermo Electron Corporation, Finland). After trypsinization, the cells were washed twice using Hank's balanced salt solution (HBS, 120 mM NaCl, 2 mM KCl, 2 mM $CaCl_2$, 2 mM $MgCl_2$, 10 mM HEPES, pH 7.4) and incubated for 1 h with fluorescent dye Fluo-4/AM (5 μg/mL; Molecular Probes, Invitrogen, Merelbeke Belgium). The cells were rinsed twice with HBS, and 100 μL of the resulting cell suspension in HBS buffer was introduced into each well of a 96-well plate (density of 150 000 cells/well). The evaluated compounds were applied at various concentrations (from 10^{-11} M to 3 × 10^{-3} M, with maximal DMSO concentration = 1%). After shaking the plate for 30 s at 1200 rpm, the emission was read at 538 nm after an excitation at 485 nm during 500 ms per measure. Measurement of a vehicle control was followed by injection of a 10 mM L-glutamate solution (10 μL), a fluorescence measurement (2 min), 15 s of shaking at 1200 rpm, and a final fluorescence measurement (5 min). The results are expressed as the EC_{50} value, which is the concentration required to reach half of the maximal intensity, and are calculated by nonlinear regression analysis (GraphPad Prism software) from at least three independent concentration−response curves made in triplicate.

Molecular modeling.

The cocrystal structure of monomer 6 with GluA2$_o$-LBD-L504Y-N775S (PDB code 4N07) was used in the docking study. The target protein was prepared with Discovery Studio 4.0, while the docking procedure was carried out with the automated GOLD 5.3.0 program.[44] The binding site was defined as a 10 Å sphere starting from the two monomers 6 in the crystal structure, allowing the incorporation of both monomers as well as the amino acids interacting with them. Potential dimeric compounds were sketched with ChemDraw (PerkinElmer Informatics) and prepared for docking with Discovery Studio 4.0 (Accelrys Inc., San Diego, California, USA). For each ligand, the number of genetic algorithm (GA) runs was set at 100. The default ChemPLP score function was used, and the search efficiency was fixed at 200%. For the output, we asked GOLD to keep the 20 best solutions for each ligand. From these solutions, clusters based on the orientation adopted by the docking poses were identified. From the cluster having the highest occurrence,

Published in : Journal of Medicinal Chemistry (2018), vol. 61, issue 12, pp. 5279-5291
doi.org/10.1021/acs.jmedchem.8b00250
Status : Postprint (Author's version)

we kept the best representative (higher PLP fitness score). This representative was then used for the minimization in situ and free binding energy calculation. The in situ minimization, free binding energy calculations, and interactions visualization were performed with Discovery Studio (DS) 4.0 (Accelrys Inc., San Diego, California, USA). The in situ minimization and free binding energy calculation were launched in the same DS protocol. In this protocol, the ligand conformational entropy[45,46] was also considered (conformers generated with the BEST algorithm), and generalized Born with molecular volume (GBMV) was used as implicit solvent model.

Crystallography.

GluA2$_o$-LBD was expressed and purified as previously described.[47] A suspension of 16 in buffer with glutamate and 10% DMSO (5 mM L-glutamate, 20 mM 16, 10 mM HEPES (pH 7.0), 20 mM NaCl, 1 mM EDTA, 10% DMSO) was mixed using shaking in the cold room overnight. Then, to the GluA2$_o$-LBD solution (in 10 mM HEPES (pH 7.0), 20 mM NaCl, 1 mM EDTA) was added 16 suspension to a resulting concentration of 5 mg/mL protein and 7 mM 16 suspension. The protein−ligand suspension was left at 6 °C for 4 days with periodic shaking. The hanging drop vapor diffusion method was used for crystallization of the complex at 6 °C. The drops consisted of 1 μL of protein−ligand solution and 1 μL of reservoir solution. The reservoir volume was 0.5 mL. The crystal used for data collection was obtained using a reservoir solution consisting of 15% PEG4000, 0.3 M ammonium sulfate, 0.1 M phosphate-citrate buffer pH 4.5. The crystal was cryo-protected using reservoir solution containing 20% glycerol before flash-cooling in liquid nitrogen.

X-ray diffraction data were collected at BioMAX, MAX IV, Lund, Sweden to a resolution of 1.4 Å. The data were processed with XDS[48] and scaled using SCALA[49] in CCP4.[50] The structure was solved with molecular replacement using PHASER[51] in CCP4, with the structure of GluA2$_o$-L504Y-N775S-LBD in complex with glutamate and 6 as search model (PDB code 4N07, chain A). The structure was built with AUTOBUILD[52] in PHENIX.[53] The program MAESTRO [version

10.1.013, Schrödinger, LLC, New York, NY, 2015] was used to generate coordinate file for compound 16. The energy minimization and conformational search were calculated in water. The parameter file of 16 was obtained using eLBOW,[54] keeping the geometry obtained from MAESTRO. The structure was manually adjusted in COOT[55] and refined in PHENIX with individual isotropic B-factors in the initial refinements and anisotropic B-factors at the final refinements, as well as riding H atoms. The structure validation was done using tools in COOT, MolProbity[56] in PHENIX, and the wwPDB Validation Service. The LBD domain closure induced by 16 was calculated using the DynDom server[57] relative to the apo structure of GluA2$_o$LBD (PDB code 1FTO, chain A). Figure 4 was made in PyMOL [version 2.0.3, The PyMOL Molecular Graphics Systems, V.S., LLC].

Associated content

* Supporting Information

The Supporting Information is available free of charge on the ACS Publications website at DOI: 10.1021/acs.jmedchem.8b00250.

Docking studies: proposed structures for docking studies, docking data and modulator-receptor interactions for selected compounds with the dimeric GluA2$_o$-LBDL483Y−N754S, interactions figures for selected compounds with the dimeric GluA2$_o$-LBD-L483Y-N754S (PDF)

Published in : Journal of Medicinal Chemistry (2018), vol. 61, issue 12, pp. 5279-5291
doi.org/10.1021/acs.jmedchem.8b00250
Status : Postprint (Author's version)

PDB code 6FAZ (PDB)
Molecular formula strings (CSV)

Author information

Corresponding Authors

*E-mail: b.pirotte@uliege.be. Phone: +32 4 366 43 65. Fax: +32 4 366 43 62.
*E-mail: lionel.pochet@unamur.be (molecular modeling).
*E-mail: j.hanson@uliege.be (pharmacological evaluation).
*E-mail: jsk@sund.ku.dk (structure determination).

ORCID

Pierre Francotte: 0000-0001-9252-7798
Jette Sandholm Kastrup: 0000-0003-2654-1510
Bernard Pirotte: 0000-0001-8251-8257

Notes

The authors declare no competing financial interest.

Acknowledgments

This work was supported by the Fonds L. Fredericq from the University of Liege and by the Fonds National de la Recherche Scientifique (F.N.R.S.), from which T.D. is a Research Fellow, P.G. is a Télévie Ph.D. Fellow, and J.H. is a Research Associate. We also acknowledge funding from The Danish Council for Independent Research/Natural Sciences (to S.L., J.S.K.), Danscatt (to L.N., S.L., J.S.K.), and CoNeXT (to L.N., S.L., J.S.K.). The technical assistance of S. Counerotte (elemental analyses) and H. Peterson (expression, purification and crystallization of GluA2$_o$-LBD) is gratefully acknowledged. We would also like to thank beamline scientists at BioMAX, MAX IV, Lund, Sweden for excellent help during data collection.

Abbreviations

ADHD, attention deficit hyperactivity disorder; AMPA, α-amino-3-hydroxy-5-methyl-4-isoxazolepropionic acid; AMPApam, positive allosteric modulator of the AMPA receptor; AMPAR, AMPA receptor; ATD, amino-terminal domain; BBB, blood−brain barrier; BTD, 1,2,4-benzothiadiazine 1,1-dioxide; CNS, central nervous system; CTD, carboxy-terminal domain; DMEM, Dulbecco's modified Eagle's medium; DMSO, dimethyl sulfoxide; FBS, fetal bovine serum; GA, generic algorithm; GBMV, generalized Born with molecular volume; HC, Hill coefficient; HBS, Hank's balanced salt; HEK cells, human embryonic kidney cells; iGluRs, ionotropic glutamate receptors; KA, kainic acid; LBD, ligand-binding domain; mGluRs, metabotropic glutamate receptors; NMDA, *N*-methyl-D-aspartic acid; NMR, nuclear magnetic resonance; SAR, structure−activity relationships; TMD, transmembrane domain; TMS, tetramethylsilane

References

(1) Kew, J. N. C.; Kemp, J. A. Ionotropic and Metabotropic Glutamate Receptor Structure and Pharmacology. *Psychopharmacol*. 2005, 179, 4−29.

Published in : Journal of Medicinal Chemistry (2018), vol. 61, issue 12, pp. 5279-5291
doi.org/10.1021/acs.jmedchem.8b00250
Status : Postprint (Author's version)

(2) Traynelis, S. F.; Wollmuth, L. P.; McBain, C. J.; Menniti, F. S.; Vance, K. M.; Ogden, K. K.; Hansen, K. B.; Yuan, H.; Myers, S. J.; Dingledine, R. Glutamate Receptor Ion Channels: Structure, Regulation, and Function. *Pharmacol. Rev*. 2010, 62, 405−496.

(3) Bassani, S.; Valnegri, P.; Beretta, F.; Passafaro, M. The GLUR2 Subunit of AMPA Receptors: Synaptic Role. *Neuroscience* 2009, 158, 55−61.

(4) Bettler, B.; Mulle, C. Review: Neurotransmitter Receptors II. AMPA and Kainate Receptors. *Neuropharmacology* 1995, 34, 123−139.

(5) Kumar, J.; Mayer, M. L. Functional Insights from Glutamate Receptor Ion Channel Structures. *Annu. Rev. Physiol*. 2013, 75, 313− 337.

(6) Carlson, G. C. Glutamate Receptor Dysfunction and Drug Targets Across Models of Autism Spectrum Disorders. Pharmacol., *Biochem. Behav*. 2012, 100, 850−854.

(7) Chang, P. K. Y.; Verbich, D.; McKinney, R. A. AMPA Receptors as Drug Targets in Neurological Disease - Advantages, Caveats, and Future Outlook. *Eur. J. Neurosci* 2012, 35, 1908−1916.

(8) Henley, J. M.; Wilkinson, K. A. Synaptic AMPA Receptor Composition in Development, Plasticity and Disease. *Nat. Rev. Neurosci*. 2016, 17, 337−350.

(9) Kristensen, B. W.; Noraberg, J.; Zimmer, J. Comparison of Excitotoxic Profiles of ATPA, AMPA, KA and NMDA in Organotypic Hippocampal Slice Cultures. *Brain Res*. 2001, 917, 21−44.

(10) Sobolevsky, A. I. Structure and Gating of Tetrameric Glutamate Receptors. *J. Physiol*. 2015, 593, 29−38.

(11) Greger, I. H.; Esteban, J. A. AMPA Receptor Biogenesis and Trafficking. *Curr. Opin. Neurobiol.* 2007, 17, 289−297.

(12) Herguedas, B.; García-Nafría, J.; Cais, O.; Fernández-Leiro, R., Krieger, J.; Ho, H.; Greger, I. H. Structure and Organization of Heteromeric AMPA-type Glutamate Receptors. *Science* 2016, 352, 549−559.

(13) Greger, I. H.; Watson, J. F.; Cull-Candy, S. G. Structural and Functional Architecture of AMPA-Type Glutamate Receptors and Their Auxiliary Proteins. *Neuron* 2017, 94, 713−730.

(14) Sobolevsky, A. I.; Rosconi, M. P.; Gouaux, E. X-ray Structure, Symmetry and Mechanism of an AMPA-subtype Glutamate Receptor. *Nature* 2009, 462, 745−756.

(15) Weeks, A. M.; Harms, J. E.; Partin, K. M.; Benveniste, M. Functional Insight into Development of Positive Allosteric Modulators of AMPA Receptors. *Neuropharmacology* 2014, 85, 57−66.

(16) Jin, R.; Clark, S.; Weeks, A. M.; Dudman, J. T.; Gouaux, E.; Partin, K. M. Mechanism of Positive Allosteric Modulators Acting on AMPA Receptors. *J. Neurosci*. 2005, 25, 9027−9036.

(17) Meyerson, J. R.; Kumar, J.; Chittori, S.; Rao, P.; Pierson, J.; Bartesaghi, A.; Mayer, M. L.; Subramaniam, S. Structural Mechanism of Glutamate Receptor Activation and Desensitization. *Nature* 2014, 514, 328−334.

(18) Ptak, C. P.; Ahmed, A. H.; Oswald, R. E. Probing the Allosteric Modulator Binding Site of GluR2 with Thiazide Derivatives. *Biochemistry* 2009, 48, 8594−8602.

(19) Ptak, C. P.; Hsieh, C.-L.; Weiland, G. A.; Oswald, R. E. Role of Stoichiometry in the Dimer-stabilizing Effect of AMPA Receptor Allosteric Modulators. *ACS Chem. Biol.* 2014, 9, 128−133.

(20) Pirotte, B.; Francotte, P.; Goffin, E.; de Tullio, P. AMPA Receptor Positive Allosteric Modulators: a Patent Review. *Expert Opin. Ther. Pat*. 2013, 2, 615−628.

(21) Schvartz, N.; Torosdag, S.; Fertig, H.; Fletcher, L., Jr; Quan, R. B.; Schwartz, M. S.; Bryant, J. M. Cyclothiazide, a New Diureticantihypertensive Drug. *Curr. Ther. Res. Clin. Exp*. 1962, 4, 437−440.

(22) Bertolino, M.; Baraldi, M.; Parenti, C.; Braghiroli, D.; DiBella, M.; Vicini, S.; Costa, E. Modulation of AMPA/kainate Receptors by Analogues of Diazoxide and Cyclothiazide in Thin Slices of Rat Hippocampus. *Receptors Channels* 1993, 1, 267−278.

(23) Zivkovic, I.; Thompson, D. M.; Bertolino, M.; Uzunov, D.; DiBella, M.; Costa, E.; Guidotti, A. 7-Chloro-3-methyl-3−4-dihydro2H-1,2,4 benzothiadiazine S,S-dioxide (IDRA 21): a Benzothiadiazine Derivative that Enhances Cognition by Attenuating DL-alpha-amino2,3-dihydro-5-methyl-3-oxo-4-isoxazolepropanoic acid (AMPA) Receptor Desensitization. *J. Pharmacol. Exp. Ther.* 1995, 272, 300−309.

(24) Thompson, D. M.; Guidotti, A.; DiBella, M.; Costa, E. 7Chloro-3-methyl-3,4-dihydro-2H-1,2,4-benzothiadiazine S,S-dioxide (IDRA 21), a Congener of Aniracetam, Potently Abates Pharmacologically Induced Cognitive Impairments in Patas Monkeys. *Proc. Natl. Acad. Sci. U. S. A*. 1995, 92, 7667−7671.

(25) Pirotte, B.; Francotte, P.; Goffin, E.; Fraikin, P.; Danober, L.; Lesur, B.; Botez, I.; Caignard, D. H.; Lestage, P.; de Tullio, P. Ringfused Thiadiazines as Core Structures for the Development of Potent AMPA Receptor Potentiators. *Curr. Med. Chem*. 2010, 17, 3575−3582.

(26) (26) Goffin, E.; Drapier, T.; Probst Larsen, A.; Geubelle, P.; Ptak, C. P.; Laulumaa, S.; Rovinskaja, K.; Gilissen, J.; de Tullio, P.; Olsen, L.; Frydenvang, K.; Pirotte, B.; Hanson, J.; Oswald, R. E.; Kastrup, S. J.; Francotte, P. 7-Phenoxy-Substituted 3,4-Dihydro-2H-1,2,4-benzothiadiazine 1,1-Dioxides as Positive Allosteric Modulators of α-Amino-3hydroxy-5-methyl-4-isoxazolepropionic Acid (AMPA) Receptors with Nanomolar Potency. *J. Med. Chem*. 2018, 61, 251−264.

(27) Kaae, B. H.; Harpsøe, K.; Kastrup, J. S.; Sanz, A. C.; Pickering, D. S.; Metzler, B.; Clausen, R. P.; Gajhede, M.; Sauerberg, P.; Liljefors, T.; madsen, U. Structural Proof of a Dimeric Positive Modulator Bridging Two Identical AMPA Receptor-Binding Sites. *Chem. Biol.* 2007, 14, 1294−1303.

(28) Krintel, C.; Frydenvang, K.; Olsen, L.; Kristensen, M. T.; de Barrios, O.; Naur, P.; Francotte, P.; Pirotte, B.; Gajhede, M.; Kastrup, J. S. Thermodynamics and Structural Analysis of Positive Allosteric Modulation of the Ionotropic Glutamate Receptor GluA2. *Biochem. J.* 2012, 441, 173−178.

(29) Nørholm, A.-B.; Francotte, P.; Olsen, L.; Krintel, C.; Frydenvang, K.; Goffin, E.; Challal, S.; Danober, L.; Botez-Pop, I.; Lestage, P.; Pirotte, B.; Kastrup, J. S. Synthesis, Pharmacological and Structural Characterization, and Thermodynamic Aspects of GluA2Positive Allosteric Modulators with a 3,4-Dihydro-2H-1,2,4-benzothiadiazine 1,1-Dioxide Scaffold. *J. Med. Chem.* 2013, 56, 8736−8745.

(30) Francotte, P.; Nørholm, A. B.; Deva, T.; Olsen, L.; Frydenvang, K.; Goffin, E.; Fraikin, P.; de Tullio, P.; Challal, S.; Thomas, J.-Y.; Iop, F.; Louis, C.; Botez-Pop, I.; Lestage, P.; Danober, L.; Kastrup, J. S.; Pirotte, B. Positive Allosteric Modulators of 2-Amino-3-(3-hydroxy-5methylisoxazol-4-yl)propionic Acid Receptors Belonging to 4-Cyclopropyl-3,4-dihydro-2H-1,2,4-pyridothiadiazine Dioxides and Diversely Chloro-substituted 4-Cyclopropyl-3,4-dihydro-2H-1,2,4-benzothiadiazine 1,1-Dioxides. *J. Med. Chem*. 2014, 57, 9539−9553.

(31) Nørholm, A. B.; Francotte, P.; Goffin, E.; Botez, I.; Danober, L.; Lestage, P.; Pirotte, B.; Kastrup, J. S.; Olsen, L.; Oostenbrink, C. Thermodynamic Characterization of New Positive Allosteric Modulators Binding to the Glutamate Receptor A2 Ligand-binding Domain: Combining Experimental and Computational Methods Unravels Differences in Driving Forces. *J. Chem. Inf. Model.* 2014, 54, 3404− 3416.

(32) Larsen, A. P.; Francotte, P.; Frydenvang, K.; Tapken, D.; Goffin, E.; Fraikin, P.; Caignard, D. H.; Lestage, P.; Danober, L.; Pirotte, B.; Kastrup, J. S. Synthesis and Pharmacology of Mono-, Di-, and TrialkylSubstituted 7-Chloro-3,4-dihydro-2H-1,2,4-benzothiadiazine 1,1-Dioxides Combined with X-ray Structure Analysis to Understand the Unexpected Structure-Activity Relationship at AMPA Receptors. *ACS Chem. Neurosci*. 2016, 7, 378−390.

(33) Krintel, C.; Francotte, P.; Pickering, D. S.; Juknaitė, L.; Pøhlsgaard, J.; Olsen, L.; Frydenvang, K.; Goffin, E.; Pirotte, B.; Kastrup, J. S. Enthalpy-Entropy Compensation in the Binding of Modulators at Ionotropic Glutamate Receptor GluA2. *Biophys. J.* 2016, 110, 2397−2406.

(34) Francotte, P.; de Tullio, P.; Goffin, E.; Dintilhac, G.; Graindorge, E.; Fraikin, P.; Lestage, P.; Danober, L.; Thomas, J.-Y.; Caignard, D.-H.; Pirotte, B. Design, Synthesis, and Pharmacology of Novel 7-Substituted 3,4-Dihydro-2H-1,2,4-benzothiadiazine 1,1-Dioxides as Positive Allosteric Modulators of AMPA Receptors. *J. Med. Chem*. 2007, 50, 3153−3157.

(35) Girard, Y.; Atkinson, J. G.; Rokach, J. A New Synthesis of 1,2,4Benzothiadiazines and a Selective Preparation of *o*-Aminobenzenesulphonamides. *J. Chem. Soc., Perkin Trans.* 1 1979, 1, 1043−1047.

(36) Meerwein, H.; Dittmar, G.; Göllner, R.; Hafner, K.; Mensch, F.; Steinfort, O. Untersuchungen über aromatische Diazoverbindungen, II. Verfahren zur Herstellung Aromatischer Sulfonsaurechloride, Einë Neue Modifikation der Sandmeyerschen Reaktion. *Chem. Ber*. 1957, 90, 841−852.

(37) Varney, M. A.; Rao, S. P.; Jachec, C.; Deal, C.; Hess, S. D.; Daggett, L. P.; Lin, F.-F.; Johnson, E. C.; Veliçelebi, G. Pharmacological Characterization of the Human Ionotropic Glutamate Receptor Subtype GluR3 Stably Expressed in Mammalian Cells. *J. Pharmacol. Exp. Ther*. 1998, 285, 358−370.

(38) Weiss, J. N. The Hill Equation Revisited: Uses and Misuses. *FASEB J.* 1997, 11, 835−841.

(39) Priel, A.; Selak, S.; Lerma, J.; Stern-Bach, Y. Block of Kainate Receptor Desensitization Uncovers a Key Trafficking Checkpoint. *Neuron* 2006, 52, 1037−1046.

(40) Weston, M. C.; Schuck, P.; Ghosal, A.; Rosenmund, C.; Mayer, M. L. Conformational Restriction Blocks Glutamate Receptor Desensitization. *Nat. Struct. Mol. Biol.* 2006, 13, 1120−1127.

(41) Armstrong, N.; Jasti, J.; Beich-Frandsen, M.; Gouaux, E. Measurement of Conformational Changes accompanying Desensitization in an Ionotropic Glutamate Receptor. *Cell* 2006, 127, 85−97.

(42) Pøhlsgaard, J.; Frydenvang, K.; Madsen, U.; Kastrup, J. S. Lessons from more than 80 Structures of the GluA2 Ligand-Binding Domain in Complex with Agonists, Antagonists and Allosteric Modulators. *Neuropharmacology* 2011, 60, 135−150.

(43) Topliss, J. G.; Sherlock, M. H.; Leroy, H. R.; Konzelman, L. M.; Shapiro, E. P.; Pettersen, B. W.; Schneider, H.; Sperber, N. Antihypertensive agents. I. Nondiuretic 2H-1,2,4-benzothiadiazine 1,1-dioxides. *J. Med. Chem.* 1963, 6, 122−127.

(44) Jones, G.; Willett, P.; Glen, R. C.; Leach, A. R.; Taylor, R. Development and Validation of a Genetic Algorithm for Flexible Docking. *J. Mol. Biol.* 1997, 267, 727−748.

(45) Sakkiah, S.; Arooj, M.; Kumar, M. R.; Eom, S. H.; Lee, K. W. Identification of Inhibitor Binding Site in Human Sirtuin 2 Using Molecular Docking and Dynamics Simulations. *PLoS One* 2013, 8, e51429.

(46) Tirado-Rives, J.; Jorgensen, W. L. Contribution of Conformer Focusing to the Uncertainty in Predicting Free Energies for Proteinligand Binding. *J. Med. Chem.* 2006, 49, 5880−5884.

(47) Krintel, C.; Frydenvang, K.; Ceravalls de Rabassa, A.; Kaern, A. M.; Gajhede, M.; Pickering, D. S.; Kastrup, J. S. L-Asp is a Useful Tool in the Purification of the Ionotropic Glutamate Receptor A2 LigandBinding Domain. *FEBS J.* 2014, 281, 2422−2430.

(48) Kabsch, W. XDS. *Acta Crystallogr., Sect. D: Biol. Crystallogr.* 2010, 66, 125−132.

(49) Evans, P. R. An Introduction to Data Reduction: Space-Group Determination, Scaling and Intensity Statistics. *Acta Crystallogr., Sect. D: Biol. Crystallogr*. 2011, 67, 282−292.

(50) Winn, M. D.; Ballard, C. C.; Cowtan, K. D.; Dodson, E. J.; Emsley, P.; Evans, P. R.; Keegan, R. M.; Krissinel, E. B.; Leslie, A. G.; McCoy, A.; McNicholas, S. J.; Murshudov, G. N.; Pannu, N. S.; Potterton, E. A.; Powell, H. R.; Read, R. J.; Vagin, A.; Wilson, K. S. Overview of the CCP4 Suite and Current Developments. *Acta Crystallogr., Sect. D: Biol. Crystallogr*. 2011, 67, 235−242.

(51) McCoy, A. J.; Grosse-Kunstleve, R. W.; Adams, P. D.; Winn, M. D.; Storoni, L. C.; Read, R. J. Phaser Crystallographic Software. *J. Appl. Crystallogr.* 2007, 40, 658−674.

(52) Terwilliger, T. C.; Grosse-Kunstleve, R. W.; Afonine, P. V.; Moriarty, N. W.; Zwart, P. H.; Hung, L.-W.; Read, R. J.; Adams, P. D. Iterative Model Building, Structure Refinement and Density Modification with the PHENIX AutoBuild Wizard. *Acta Crystallogr., Sect. D: Biol. Crystallogr.* 2008, D64, 61−69.

(53) Adams, P. D.; Afonine, P. V.; Bunkóczi, G.; Chen, V. B.; Davis, I. W.; Echols, N.; Headd, J. J.; Hung, L. W.; Kapral, G. J.; GrosseKunstleve, R. W.; McCoy, A. J.; Moriarty, N. W.; Oeffner, R.; Read, R. J.; Richardson, D. C.; Richardson, J. S.; Terwilliger, T. C.; Zwart, P. H. PHENIX: a Comprehensive Python-Based System for Macromolecular Structure Solution. *Acta Crystallogr., Sect. D: Biol. Crystallogr.* 2010, 66, 213−221.

(54) Moriarty, N. W.; Grosse-Kunstleve, R. W.; Adams, P. D. Electronic Ligand Builder and Optimization Workbench (eLBOW): a Tool for Ligand Coordinate and Restraint Generation. *Acta Crystallogr., Sect. D: Biol. Crystallogr.* 2009, 65, 1074−1080.

(55) Emsley, P.; Lohkamp, B.; Scott, W. G.; Cowtan, K. Features and Development of Coot. *Acta Crystallogr., Sect. D: Biol. Crystallogr.* 2010, 66, 486−501.

(56) Davis, I. W.; Leaver-Fay, A.; Chen, V. B.; Block, J. N.; Kapral, G. J.; Wang, X.; Murray, L. W.; Arendall, W. B.; Snoeyink, J.; Richardson, J. S.; Richardson, D. C. MolProbity: All-Atom Contacts and Structure Validation for Proteins and Nucleic Acids. *Nucleic Acids Res*. 2007, 35, W375−W383.

(57) Hayward, S.; Berendsen, H. J. C. Systematic Analysis of Domain Motions in Proteins from Conformational Change; New Results on Citrate Synthase and T4 Lysozyme. *Proteins: Struct., Funct., Genet*. 1998, 30, 144−154.

(58) Battisti, U. M.; Jozwiak, K.; Cannazza, G.; Puia, G.; Stocca, G.; Braghiroli, D.; Parenti, C.; Brasili, L.; Carrozzo, M. M.; Citti, C.; Troisi, L. 5-Arylbenzothiadiazine Type Compounds as Positive Allosteric Modulators of AMPA/Kainate Receptors. *ACS Med. Chem. Lett*. 2012, 3, 25−29.

(59) Halgren, T. A. Merck Molecular Force Field. I. Basis, Form, Scope, Parameterization, and Performance of MMFF94. *J. Comput. Chem.* 1996, 17, 490−519.